# QUANTIFICATION OF GENE EXPRESSION IN *AGROSTIS* SPECIES SUBJECTED TO ZINC DEFICIENCY

by
ÖZGE CANLI

Submitted to the Graduate School of Engineering and Natural Sciences
in partial fulfillment of
the requirements for the degree of
Master of Science

Sabanci University
Spring 2006-2007

QUANTIFICATION OF GENE EXPRESSION IN AGROSTIS SPECIES SUBJECTED TO ZINC DEFICIENCY

APPROVED BY:

Assoc. Prof. Dr. Hikmet BUDAK ..... (Thesis Advisor)

Prof. Dr. İsmail ÇAKMAK ..... (Thesis Co-advisor)

Prof. Dr. Zehra SAYERS .....

Prof. Dr. Selim ÇETİNER .....

Prof. Dr. Haluk ERTAN .....

DATE OF APPROVAL: .....

QUANTIFICATION OF GENE EXPRESSION IN *AGROSTIS* SPECIES SUBJECTED TO ZINC DEFICIENCY

Özge Canli

BIO, Master Thesis, 2007

Thesis Supervisor: Assoc. Prof. Dr. Hikmet BUDAK

Keywords: mRNADD, Agrostis, bentgrass, ZIP zinc transporter family, zinc deficiency

Abstract

Zinc is an essential micronutrient involved in many cellular mechanisms in biologycal systems and its deficiency causes severe reductions in crop yield and human health.

In this study, our goal is to identify and characterize the genes expressed in three *Agrostis* species; Creeping (*Agrostis stolonifera*), Colonial (*Agrostis capillaris*) and Velvet (*Agrostis canina*) bentgrass upon exposure to zinc deficiency using mRNA differential display method. Differentially expressed fragments were sequenced and analyzed further. Nine differentially expressed genes whose expression levels either increased or decreased in response to zinc deficiency were identified. Transcripts identified have partial similarities to the previously identified metal binding proteins. A full sequence of differentially expressed gene was obtained by using rapid amplification of cDNA ends (RACE) method. The expression level of this gene was quantified by Real-Time PCR and a down-regulation was observed under zinc deficiency. The identified protein was characterized based on its similarity to the ZIP family transporters. This is the first report to identify and characterize homologous of the ZIP family transporters in *Agrostis* species.

# ÇİNKO NOKSANLIĞİNDA *AGROSTIS* TÜRLERİNDEKİ GEN ESPRESYONUNUN SEVİYESİNİN BELİRLENMESİ

Özge CANLI

BIO, Yüksek Lisans Tezi, 2007

Tez Danışmanı: Doç. Dr. Hikmet BUDAK

Anahtar Kelimeler: mRNADD, Agrostis, ZIP gen ailesi, çinko noksanlığı

## Özet

Çinko, biyolojik sistemlerde, birçok hücresel mekanizmada rol alan temel bir mikrobesindir ve çinkonun, eksikliğinde, bitkisel verim ve insan sağlığında problemler ortaya çikar .

Bu çalışmadaki amacımız, üç farklı Agrostis türünde; Creeping (*Agrostis stolonifera*), Colonial (*Agrostis capillaris*) ve Velvet (*Agrostis canina*) bentgrass, mRNADD metodu kullanarak, çinko noksanlığındaki gen ekspresyon profilini görüntülemekti. Farklı ekspresyon seviyesine sahip genler, sekanslandı ve analiz edildi. Ekspresyonu, çinko noksanlığında azalan veya artan dokuz gen tespit edildi. Elde edilen diziler, bilinen metal bağlayan proteinlerle kısmi benzerlikler gösterdi. RACE metodu kullanılarak, bu genlerden birinin tüm mRNA sekansı elde edildi. Bu genin ekspresyon seviyesindeki farklılık, gerçek zamanlı PCR metoduyla belirlendi ve çinko noksanlığında, ekspresyon seviyesinde belirgin bir düşüş gözlemlendi. Genin kodladığı protein, ZIP taşıyıcı gen ailesiyle gösterdiği benzerliklere dayanarak karakterize edildi. Bu çalışma sonucunda, Agrostis türlerinde ilk defa bir ZIP ailesi homoloğu belirlenmiş oldu.

# Acknowledgments

*There were times, it was challenging. I was exhausted in need of guidance, encouragement, tenderness. I deeply thank you all, for never leaving me alone...*
*Thank you;*

My adviser; *Hikmet Budak*, for your invaluable support and guidance during the completion of this thesis and for your infinite endurance.

My coadviser; *İsmail Çakmak*, for your contribution and supervision.

*Zehra Sayers*, for your advises and the genuine effort to help me find a way out when I was completely stuck.

The committee members; *Selim Çetiner* and *Haluk Ertan*, for the time you pleasantly spent to evaluate the thesis.

*Senem Su, Gizem Dinler, Neslihan Ergen* and *Fahriye Ertuğrul*, for legitimately sharing your experience.

*Atilla Yazıcı, Veli Bayır, Özgür Gökmen*, for your help in the greenhouse.

My lab mates; *Ceyda Çoruh, Zeynep Işık, Barış Kutman, Özge Cebeci* and *Burcu Köktürk*, for being there any time I needed.

*Filiz Kısaayak, Filiz Dede, Burcu Kaplan, Dilek Telci, Özgür Gül, Günseli Bayram*, for your help and support in the lab.

*Deniz Saltukoğlu, Pınar Önal, Tuğsan Tezil, Sema Kurtuluş, İbrahim Aksoylar, Işıl Nalbant, Atakan Ertuğrul, Sedef Önal, Deniz Turgut* and *Gözde Korkmaz*, nothing would have been the same without your warm presence.

My eternal friend; *Erhan Sunar*, for everything you have done in the last fifteen years.

My mentor, my adviser, my friend, my dear; *Onur Gökçe*, for breaking my sorrow with an irreplaceable intimacy and for all those long nights.

My lovely family; *Gözde Canlı, Türkan Canlı* and *Zeki Canlı*, for your ingenuous love and for your endless faith and trust.

# Contents

# List of Figures

# List of Tables

# List of Abbreviations

| | |
|---|---|
| APS | Ammonium persulphate |
| CA | Carbonic anhydrase |
| CT | Cycle threshold |
| $ddH_2O$ | Double distilled water |
| EDTA | Ethylenediaminetetraaceticacid |
| GFP | Green florescent protein |
| GST | Glutathione-s-transferase |
| ICP-OES | Inductively coupled plasma optical emission spectroscopy |
| mRNADD | mRNA differential display |
| ORF | Open reading frame |
| PAGE | Polyacrylamide gel electrophoresis |
| PCR | Polymerase chain reaction |
| PPM | Parts per million |
| RACE | Rapid amplification of cDNA ends |
| SDS | Sodium dodecyl sulphate |
| TEMED | Tetramethylethylenediamine |
| UV | Ultraviolet |
| ZIP | ZRT,IRT like protein |

# Chapter 1

# Introduction

## 1.1 Agrostis species

Grass family has a particular importance as rice, wheat and maize constitutes the major portion of dietary not only for humans but also for domestic animals. Moreover, grasses form a significant part of the urban and suburban landscape all over the world cover approximately 20% of the earth's land surface [1, 2].

Agrostis genus of the Poaceae family, consists of more than 200 species. Three bentgrasses, namely Creeping bentgrass (*Agrostis stolonifera*), Colonial bentgrass (*Agrostis capillaris*) and Velvet bentgrass (*Agrostis canina*), are the most commonly used in earth's landscape especially in athletic fields and golf courses [3, 4]. Among those three, creeping bentgrass is the most commercially important bentgrass used especially in golf course due its fine leaves and tolerance to low cutting heights [5].

Agrostis species are used in many research to study herbicide resistance, heavy metal tolerance and other various aspects. One of the earliest research about Agrostis species and their interaction with metals published in Nature, states that *Agrostis tenuis* is resistant to lead and zinc toxicity [6]. A recent study on Agrostis species with various metals such as lead, zinc and cadmium

have verified this hypothesis and demonstrated that the interaction of two of these heavy metals on plants can be formulated in two different ways; interaction may either lead to the enhancement of toxic action resulting from the summation of toxicity or may alter the absorption or transport of toxicants in different ways depending on the metals [7].

Two recent study on creeping bentgrass, colonial bentgrass and velvet bentgrass species have provided valuable information about the transcribed genes in grass species that might be useful in comparative genome analysis [4]. There is lack of knowledge on the identification and characterization of zinc responsive genes in Agrostis species.

## 1.2 Importance of zinc for mammalians

Zinc is needed by humans in small but critical amounts however, inadequate amounts may cause disfunction of many enzymes and other metabolic functions in which zinc takes part. In developing countries, it is of great importance to increase the amount of dietary zinc. There is a global effort for micronutrient enrichment through plant breeding [8]. Succeeding in this may contribute to improving the health of many micronutrient deficient people not only in developing countries but worldwide.

### 1.2.1 Biochemistry of zinc

Zinc is one of the essential trace elements for humans. Due to its ability of strong but exchangeable ligand binding zinc was proved to be useful in biological systems [9]. Zinc has many specific structural roles in enzymes, other proteins and biomembranes. It is ubiquitous in subcellular metabolism and an essential component of the catalytic site of at least one member of any enzyme classification. [10]. So far, many zinc metalloenzymes have been

characterized in animal and plant kingdoms. A specific example for the role of zinc is the zinc finger motif which is one of most common DNA binding motifs. A single zinc atom regulates the binding of zinc fingers to the DNA. This motif exists in many transcription factors and recently similar motifs were identified in nuclear hormonal receptors [11, 12, 13]. These important roles of zinc in metabolism suggest that zinc deficiency may result in metabolic abnormalities for biosystems.

### 1.2.2 Zinc deficiency

Fundamental importance of zinc in cellular growth and differentiation was demonstrated in animal model systems especially for rapidly growing tissues and organs such as embryo [14]. In addition to this, it was found that zinc deficiency also affects tissues that are not rapidly growing or differentiating such as central nervous system [15]. It is known that zinc deficiency results in loss of appetite, inability to gain weight, skeletal abnormalities, skin lesions and hair abnormalities in growing animals [16].

The first major hypothesis about the effects of zinc deficiency on mammals, was discovered in the mid-Eastern countries for the syndrome of adolescent nutritional dwarfism [17]. Since then, many clinical research have identified divergent effects of zinc deficiency on human health. Epidermal, gastrointestinal, central nervous, immune, skeletal and reproductive systems are reported as the organ systems that are affected by zinc deficiency [13]. Growth abnormalities due to zinc deficiency is one of the most studied health problems among others and was shown to be reduced by zinc supplementation. Many other health problems such as diarrhea, pneumonia, neurological defects, childhood mortality,malaria were also overcome by increasing the amount of zinc in dietary [18].

## 1.3 Zinc in plant nutrition

Zinc is one of the eight trace elements which are essential for the normal growth and reproduction of crop plants. Zinc deficiency in soils causes severe reductions in both crop production and grain quality, as shown in different countries like in India, Turkey, China and Australia [19]. Figure 1.1 provides a list of countries that zinc deficiency was reported.

Studies with various plant species have clarified many aspects on the importance of metals and the mechanisms of metal accumulation and homeosteasis in plants. For instance, the recent study on *Medicago truncatula* predicted six new metal binding proteins with a high level of similarity to the ZIP protein family [20]. In another study on *Arabidopsis thaliana*, it was reported that cation efflux family is involved in Zn homeostasis [21].

### 1.3.1 Physiological role of zinc in plants

Zinc is an essential mineral nutrient and a cofactor of enzymes and proteins involved in many cellular mechanisms. It has a strong tendency to form tetrahedral complexes with nitrogen, oxygen and sulfur ligands and plays both a catalytic and a structural role in enzymatic reactions [22]. The predominant forms of zinc in plants are low molecular weight complexes, storage metalloproteins, free ions, and insoluble forms associated with the cell wall breaks.

Zinc can be inactivated by the formation of complexes with organic ligands or phosphorus. The water soluble fraction of zinc that is mostly found in the low molecular weight complexes is the most physiologically active form of total zinc in plants [23].

Zinc deficiency has effects on carbohydrate and protein metabolisms, membrane integrity, auxin metabolism and reproduction in plants [19]. Zinc


Figure 1.1: Countries with reported zinc deficiency [19].

has an effect on carbohydrate metabolism through its role in photosynthesis and sugar transformations [22, 24]. It has also an indirect role in protein metabolism due its necessity for the activity of enzyme RNA polymerase. Zinc deficiency triggers ribonuclease activity and causes a decrease in RNA level as a result [23]. In plants, zinc plays a critical role for the integrity of biomembranes that may involve the orientation of macromolecules and the maintenance of ion transport systems and protection of membrane proteins from the destructive effects of superoxide radicals and their derivatives produced by redox reactions within the cell [25, 26, 19]. Zinc has a regulatory effect on synthesis of auxin, a growth regulation compound. The evidence shows that zinc is required for the biosynthesis of tryptophan which is the most likely precursor of auxin [23]. In zinc deficient plants, a reduction in the seed production was observed probably due to the increased formation of abscisic acid causing premature loss of leaves and flower buds and disruption of the development and physiology of anthers and pollen grains [23, 19].

**Low molecular weight complexes of zinc**

In plants, soluble zinc occurs mainly as anionic compound and thought to be associated with amino acids whereas free zinc ions constitute only a small proportion of the soluble zinc content [23, 19]. The low molecular weight complexes of zinc such as phytochelatins that are synthesized in response to excess cadmium, zinc and mercury exposure are thought to be the most physiologically active forms of zinc [19].

**Zinc in proteins**

In plants, zinc plays a role as functional, structural and regulatory cofactor of many enzymes [19]. So far, more than 70 metalloenzymes containing zinc have been identified and found to be the members of either oxidoreductase,

transferase, hydrolase, lyase, isomerase and ligase enzyme classes [27]. The zinc atom usually binds to the apoenzyme and forms strong complexes with radicals of polar groups containing oxygen, nitrogen and sulphur [23].

X-ray analysis shows that the zinc binding pattern the enzymes is changed depending on its role. Zinc is mostly bound through imadazole or cysteine if it has a functional role. Catalytic zinc is bound with three protein ligands and a water molecule whereas in enzymes that zinc has a structural or regulatory role it is bound with four protein ligands. Depending on this fact the water molecule is considered essential for the catalytic activity of zinc [23, 19].

A very recent study suggested that the activity of CA (carbonic anhydrase), an enzyme that catalyses the the hydration of $CO_2$, is highly correlated to Zn tissue concentrations [28].

### 1.3.2 Mechanisms of zinc uptake by plants

Zinc is mostly absorbed as an ion from the soil by the roots with a protein that has a high affinity for zinc and the efficiency of zinc uptake decreases in dry soils when compared to wet soils [19, 29]. Zinc uptake was found to be pH dependent and uptake of micronutrients mutually inhibit each other possibly because the same mechanism is used for several micronutrients [30]. Zinc is accumulated in the root and translocated to the shoot as an ion or complex with organic acids when needed [19]. It was also reported that alkaline earth conditions inhibit zinc uptake at a certain level depending on the conditions [31].

Zinc is taken up from soils by root membrane transport mechanisms. The selectivity of these transporters determines whether other divalent cations are imported at the same time with zinc. Recent advances have revealed that plant genomes contain several gene families involved in the transport of di-

valent micronutrients [32]. Some of these transporters have broad substrate specificity, but the range of specificities in plant zinc transporters is unknown because their functional characterization is lagging behind the gene discovery [33]. There appears to be at least one family of transporters in plants that should be relatively specific for iron and zinc uptake; however, the precise metal ions that these transporters take up may vary according to the composition of metal ions in the environment [34, 35, 36, 37]. Although the molecular identity of specific zinc transporters has become evident in plants, we know little about how the structures of these proteins interact to create differences in functional characteristics, such as ionic selectivity. Ionic selectivity is particularly important for plant zinc transporters in root cells. In soils that contain contaminants such as cadmium, zinc transport mechanisms may allow for cadmium entry into whole plants [38, 39].

In recent years, scientist have identified various genes that encode proteins involved in membrane transport of metals and Grusak provided extensive information on the topic and how this might be used in transgenic strategies [40]. Grusak has modeled the potential control points in the regulation of metal homeostasis in crop plants (Figure 1.2). According to his model, soil particles are transported to different compartments via variable pathways through xylem, pholoem and vegatative tissues [41].

### 1.3.3 Causes of zinc deficiency

In 1972, Lindsay categorized the most important factors effecting zinc availability in soils under nine major groups; soils with low zinc content, soils with restricted root zones, calcareous soils, soils of low organic matter content, microbially inactivated zinc, low temperature soils, plant species and varieties, high levels of available phosphorous and effect of nitrogen [42]. Fig-

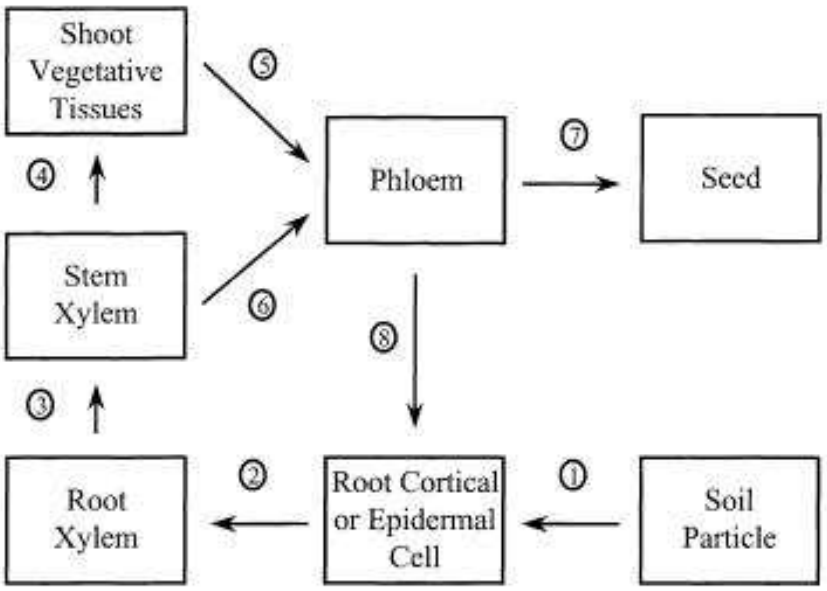


Figure 1.2: Potential control points in the regulation of metal homeostasis in crop plants. This scheme is generalized to indicate analogous steps for all micronutrients. Regulatory processes which would influence the movement of metals from one compartment to the next include: (1) root acquisition/uptake phenomena; (2) intracellular transport, including the involvement of xylem parenchyma; (3) cell-wall-cationic binding sites within the xylem pathway; (4) transpiration rates of vegetative tissues; (5) capacity for phloem loading of metal ions, including the necessity of chelators for some metals; (6) xylem-to-phloem exchange; (7) phloem transport capacity of photoassimilates from a given source region; (8) communication of shoot micronutrient status via phloem-mobile signal molecules. [41]

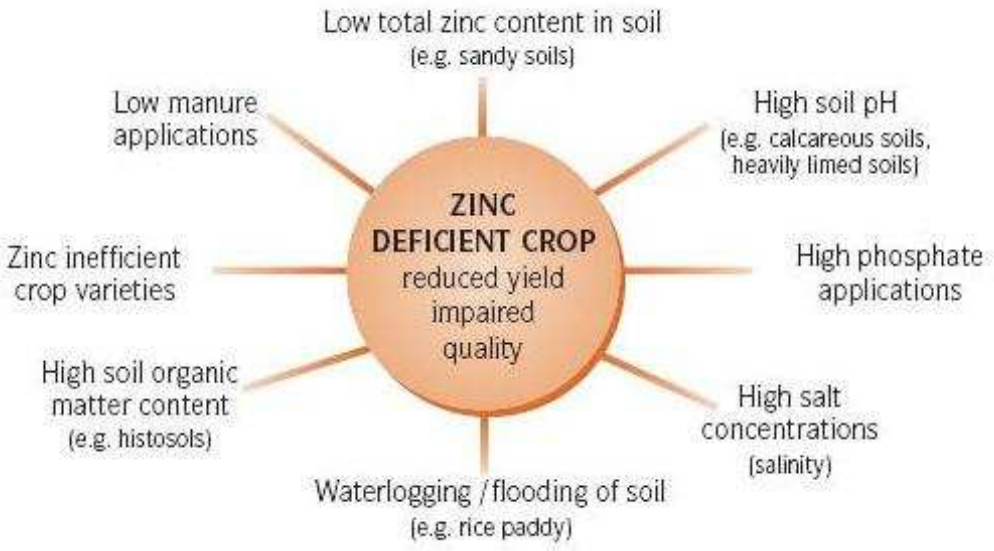


Figure 1.3: Schematic diagram of the causes of zinc deficiency in crops [19].

ure 1.3 shows Alloway's schematic description of the causes of zinc deficiency in crops.

## 1.4 The ZIP family of metal transporters

The ZIP gene family is a metal transporter family first identified in plants. Its members are transporters of a variety of cations, including cadmium, iron, manganese and zinc.

The name ZIP comes from the first members identified (ZRT, IRT-like protein) in *Arabidopsis* [43]. IRT1 is a cation transporter expressed in the roots of iron deficient plants and ZRT1 and ZRT2 are zinc transporters identified in yeast [34, 39]. Many ZIP proteins have been identified in plants, yeast, bacteria, archea, human and many other mammalians indicating that specific ZIP transporters may play different roles in metal transport [44, 45, 46].

The ZIP family can be split into several subfamilies based on a their

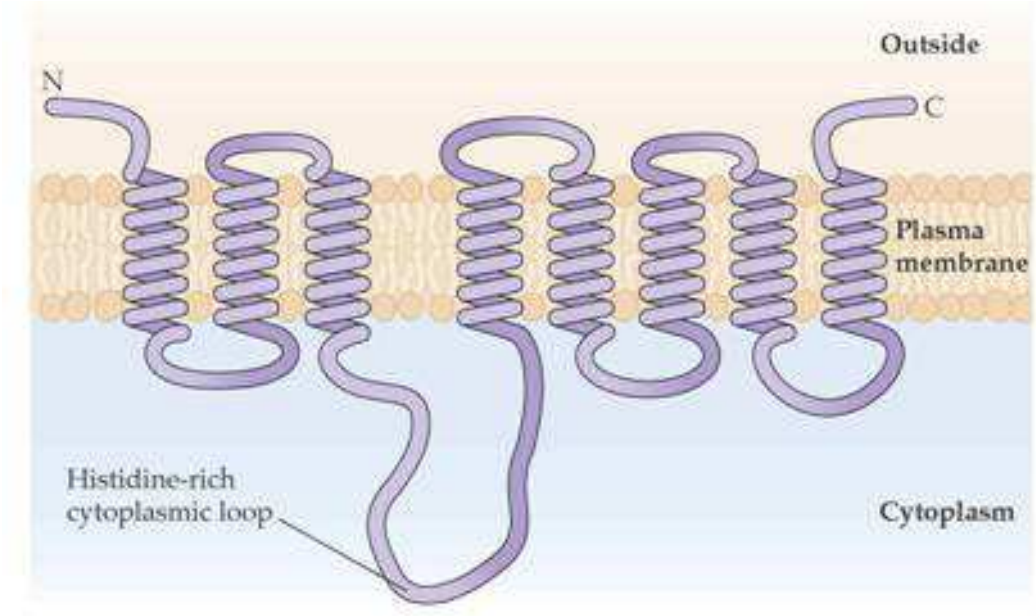


Figure 1.4: Predicted topology of ZIP family members. ZIP proteins cross the membrane eight times. There is a variable region between transmembrane domains 3 and 4 that is histidine-rich and predicted to reside in the cytoplasm [47].

sequence conservation within these groups. Most ZIP proteins have eight transmembrane domains whereas some have fewer. These domains have a similar membrane topology in which the amino- and carboxy-terminal ends of the protein are located on the outside surface of the plasma membrane and the transmembrane region is the most conserved portion of the ZIP family proteins (Figure 1.4). ZIP family proteins mostly range from 309 to 476 amino acids in length, this difference is largely due to the length between transmembrane domains [43]. Figure 1.5 shows the structure of Irt1 protein of ZIP family.

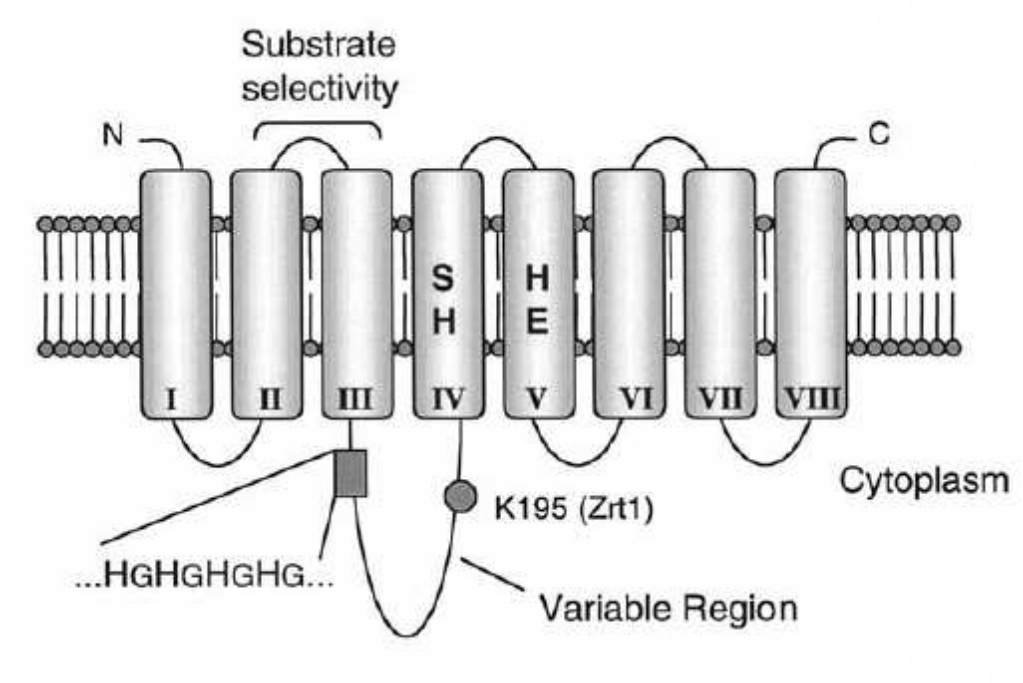


Figure 1.5: Predicted topology of Irt1. Irt1, is predicted to have eight transmembrane domains. The conserved and functionally important residues within domains V and VI are indicated as is the variable region, the ubiquitinated K195 in Zrt1, and the extracellular loop region that affects Irt1 substrate specificity [48].

## 1.5 mRNA differential display

Differential display (DD) technology is one of the major tools that was developed by Liang and Pardee to speed up the identification of differentially expressed genes [49]. The method is based on simple molecular biology tools. First, mRNAs from cells are converted to first strand cDNAs using oligo-dT primers that enable the initiation of cDNA synthesis at the beginning of poly(A) tail of any given mRNA. The cDNAs are further amplified using a set of primers that are short and arbitrary in sequence and recognizing 50-100 mRNAs [49]. The cDNAs can be visualized using gel electrophoresis and comparisons of such cDNA patterns between relevant mRNA samples reveal the differences in gene expression profiles. Figure 1.6 illustrates the basic mechanism of differential display. Differentially expressed cDNA bands can be cloned and sequenced for further analysis. Mathematical models have been proposed to predict the relationship between the number of arbitrary primers and the coverage of expressed genes in any given eukaryotic cells [50]. According to this model, a primer would recognize one twelfth of the total mRNA population because there are twelve different combinations of the last three bases.

Differential display method is used in many recent studies as a tool to obtain gene expression profiles not only of plants but also animals. In a recent study, differentially expressed genes in *Festuca rubra* upon *Puccinia* infection was identifed using mRNA differential display method [51]. In another study, 10 zinc responsive genes in fall webworm,*Hyphantria cunea* were identified using differential display method [52]. This method was also applied to durum wheat to identify cadmium responsive genes [53].

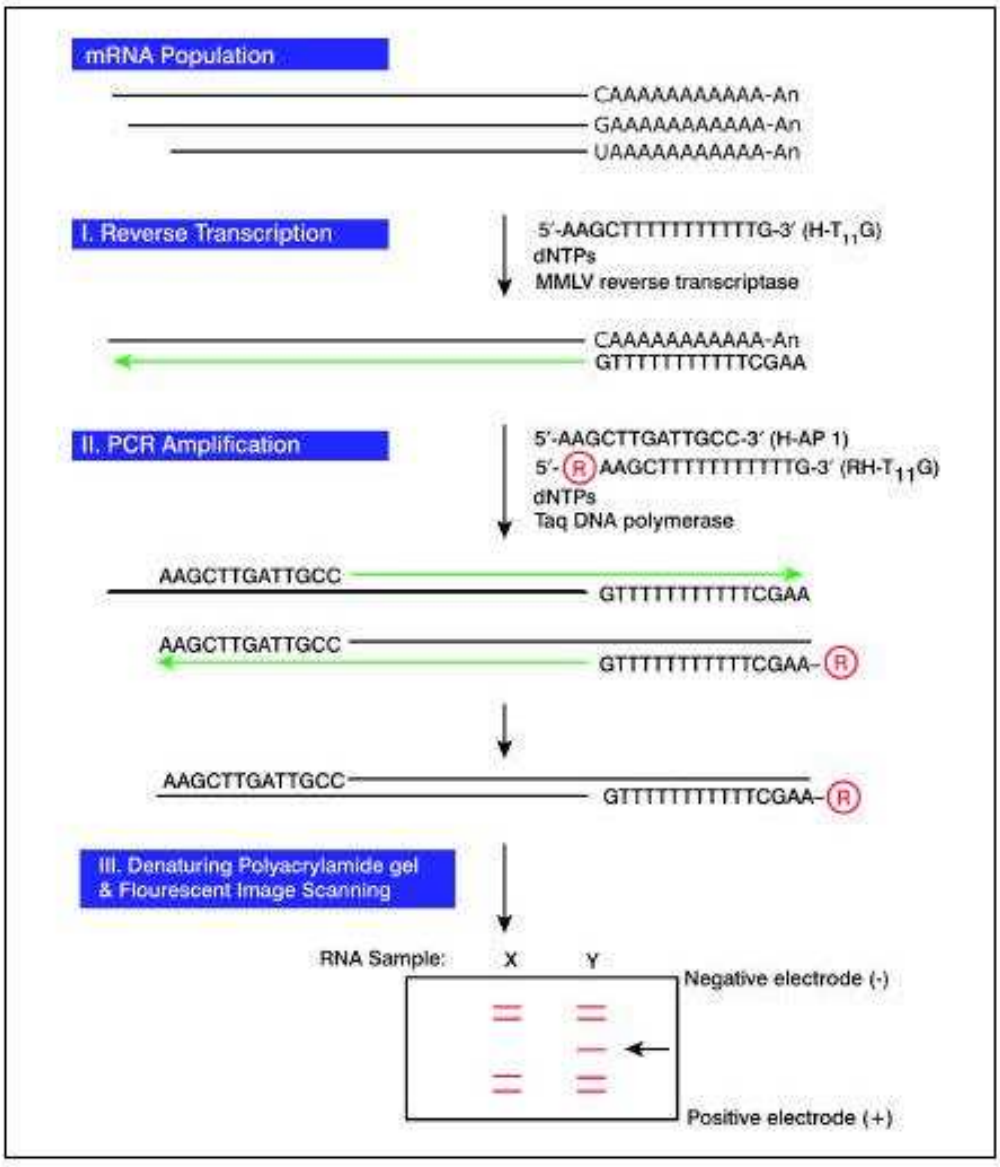


Figure 1.6: Schematic illustrations of fluorescent differential display [54].

## 1.6 Aim of the study

Because zinc is an essential micronutrient for both plants and humans, it is important to characterize zinc dependent pathways in plants. In plants, metal deficiencies cause an altered expression or function of proteins at the metabolic level and may lead to some physiological symptoms such as reduced growth [20, 55].

In this study, the gene expression profiles of three bentgrass species, Colonial, Creeping and Velvet bentgrass, were identified using mRNA differential display method in response to zinc deficiency. The plants grown under different zinc concentrations were subjected to mRNA differential display method. Differentially expressed fragments were sequenced and analyzed further. Nine differentially expressed genes were found for the three bentgrass types whose expression levels either increased or decreased in response to zinc deficiency. Majority of the identified transcripts have partial high similarities to the previously identified metal binding proteins.

The expression level of one of the novel genes that had a decreased expression pattern under zinc deficiency in Creeping bentgrass was quantified by Real-Time PCR and a dramatic decrease in the expression level of the transcript was observed under zinc deficiency. The full mRNA sequence of the transcript was obtained for the first time in Creeping bentgrass, using RACE method and this led to the identification of a ZIP family zinc transporter. The full length AsZIP was submitted to GenBank database.

# Chapter 2

# Materials and Methods

## 2.1 Materials

### 2.1.1 Chemicals and equipment

For the detailed list of chemicals and equipment that has been used during this project, please refer to Appendix A.1 and A.2.

## 2.2 Methods

### 2.2.1 Plant growth

#### Green house trial

Three parallels of Creeping bentgrass (*Agrostis stolonifera*L-93 M5-4-872-1), Colonial bentgrass (*Agrostis capillaris*SR7100 B28-6-7100-4) and Velvet bentgrass (*Agrostis canina*1-464-309) species were grown under different zinc concentrations in green house under controlled environmental conditions in 1500g soil in plastic pots. The Zn deficient soil was obtained from Central Anatolia (pH:8.04, $CaCO_3$ 14.9%, organic matter 0.69%, salt 0.08% and clay 60.6%). The basal treatment was 200 mg/kg N as $Ca(NO_3)_2$ and 100 mg/kg P as $KH_2PO_4$, 125 mg K kg-1 soil as $KH_2PO_4$, 20 mg S kg-1 soil as $CaSO_4.2H_2O$, 2.5 mg/kg F as FeEDTA ($C_10H_12FeN_2$ $NaO_8$) and 0,0.1

and 5 mg/kg Zn as $ZnSO_4.7H_2O$ applied for all species. The plants were grown for 30 days by daily water supply as deionized water. After 30 days of growth in the greenhouse, the shoots were harvested and dried at 70°C for determination of shoot dry matter production and elementary decomposition of the shoot. Also for the molecular analysis, another trial with the same basal treatment and 0 and 5mg/kg Zn as $ZnSO_4.7H_2O$ was set and the shoots were harvested after 30 days of growth and were frozen in liquid nitrogen and kept at -80°C before use.

**Tissue culture trial**

Ten seeds, after surface sterilization with 5% sodium hypochlorite for ten minutes, were planted in 20ml plant tissue culture medium containing 0 or 5ppm zinc. Plants were grown for 21 days in the growth room at 26°C and with 16:8 hours of light and dark photoperiodicity.

### 2.2.2 Shoot dry matter production and zinc analysis

**Dry Matter Production**

After four weeks of growth only shoots were harvested. Plant materials were dried at 70°C were weighed for determination of dry matter production and the dry matter per plant was calculated by dividing the total weight with the number of plants per pot.

**Element concentration and content**

The dried shoot samples were grounded and varying amount of grounded samples (0.05-0.2 g) were ashed at 500°C for 12 hours for determination of elementary concentration.

The ashed samples were dissolved in 3.3% $HNO_3$ (v/v). The concentration of zinc as well as other elements (Ca, K, P, S, Mg, Fe, Mn, Cu, Al, Na)

was measured by inductively coupled plasma optical emission spectroscopy (ICP-OES, Varian, Australia) at 214.439 nm emission wavelength.

### 2.2.3 cDNA material

#### RNA isolation

0.2 g of shoot samples was grounded with 2 mL TRIzol using mortars and pestles. The homogenized samples were incubated 5 minutes at room temperature in microtubes. 0.4 mL chloroform was added, shaken and incubated for 5 minutes in room temperature. After centrifugation at 11.000 g for 15 minutes at 4°C upper aqueous phase was transferred to clean tube. 2mL 2-propanol was added and the samples were incubated for 10 minutes on ice. RNA was precipitated by the centrifugation at 11.000 g for 10 minutes at 4°C. The pellet was washed by 2mL 75% ethanol and centrifuged at 7.500 g for 5 minutes at 4°C. RNA pellet was air-dried for 10 minutes and dissolved in 40$\mu$l formamide by incubation at 55°C for 40 minutes. The total amount of RNA was measured by a nanodrop spectrophotometer and the samples were stored at -20°C.

#### DNase treatment

RNase free DNaseI (Fermentas) was used to treat RNA samples. The reaction mix containing 1u of DNase for 2$\mu$g RNA, 1X reaction buffer and DEPC treated water was incubated at 37°C for 30 minutes. RNA was precipitated by ethanol precipitation. 0.1 volumes of 3M NaOAc ph 5.2 and 2 volumes of 100% chilled ethanol was added to the samples and incubated at -80°C for 1 hour. The supernatant was discarded after centrifugation at 4°C and the pellet was washed with 70% ethanol. After 10 minutes of air-drying the pellet was dissolved in formamide and RNA was quantified using nanodrop

spectrophotometer.

**Reverse transcription**

cDNA synthesis from the samples were performed by Omniscript Reverse Transcription kit(Qiagen). The reaction mix contained 4 units of reverse transcriptase for 1$\mu$g RNA, 0.5mM dNTP, 1X reaction buffer, 1$\mu$M oligo-dT primers, 10 units RNase inhibitor and RNase free water up to 20l final volume.

### 2.2.4 mRNA differential display

The cDNAs were subjected to mRNA differential display method by using 72 combinations of forward (P) and reverse(T) primers (Table 2.1) [49]. The PCR mix contained 500ng of cDNA template, 10$\mu$M of each primer, 0.2mM dNTP mix, 2,5mM $MgCl_2$, 1X reaction buffer and 0,2 unit Taq DNA polymerase for 25$\mu$l. Reactions were carried out in DNA thermocycler GeneAmp PCR System 9700 (PE Applied Biosystems) using the conditions in Table 2.2.

The PCR products were visualized by ethidium bromide staining after seperation by 2% agarose gel electrophoresis with TBE buffer.

### 2.2.5 Sequencing

**Gel extraction**

For gel extraction, 50$\mu$l PCR products of mRNADD were run on 2% agarose gel. The bands of interests were extracted from the gel using QIAquick Gel Extraction kit according to manufacturer's instructions.

Table 2.1: Primers used in mRNA differential display

| Primer designation | Sequence (5' - 3') |
|---|---|
| P1 | ATT AAC CCT CAC TAA ATG CTG GGG A |
| P2 | ATT AAC CCT CAC TAA ATC GGT CAT AG |
| P3 | ATT AAC CCT CAC TAA ATG CTG GTG G |
| P4 | ATT AAC CCT CAC TAA ATG CTG GTA G |
| P5 | ATT AAC CCT CAC TAA AGA TCT GAC TG |
| P6 | ATT AAC CCT CAC TAA ATG CTG GGT G |
| P7 | ATT AAC CCT CAC TAA ATG CTG TAT G |
| P9 | ATT AAC CCT CAC TAA ATG TGG CAG G |
| T1 | CAT TAT GCT GAG TGA TAT CTT TTT TTT TAA |
| T2 | CAT TAT GCT GAG TGA TAT CTT TTT TTT TAC |
| T3 | CAT TAT GCT GAG TGA TAT CTT TTT TTT TAG |
| T4 | CAT TAT GCT GAG TGA TAT CTT TTT TTT TCA |
| T5 | CAT TAT GCT GAG TGA TAT CTT TTT TTT TCC |
| T6 | CAT TAT GCT GAG TGA TAT CTT TTT TTT TCG |
| T7 | CAT TAT GCT GAG TGA TAT CTT TTT TTT TGA |
| T8 | CAT TAT GCT GAG TGA TAT CTT TTT TTT TGC |
| T9 | CAT TAT GCT GAG TGA TAT CTT TTT TTT TGG |

Table 2.2: mRNA differential display PCR

| | | Temperature (°C) | Time |
|---|---|---|---|
| | Heating Lid | 105 | hold |
| | Denaturation | 94 | 4 min |
| | Non-specific annealing | 40 | 5 min |
| | Extension | 72 | 5 min |
| 2 cycles | Denaturation | 94 | 1 min |
| | Non-specific annealing | 40 | 1 min |
| | Extension | 72 | 5 min |
| 30 cycles | Denaturation | 94 | 30 sec |
| | Annealing | 58 | 30 sec |
| | Extension | 72 | 2 min |
| | Final elongation | 72 | 7 min |

### Ligation and Transformation

The extracted fragments were ligated into PGEM-T easy vector (Promega, Madison, Wisconsin, USA) by TA cloning as described in the manufacturer's protocol using 3 to 1 vector insert ratios in 12$\mu$l ligation mix. The ligation mix was used to transform the JM109 high efficiency competent cells provided with the kit as described in PGEM-T vector manual. The transformants were grown overnight on ampicillin/IPTG/X-Gal containing media.

### Colony PCR

White colonies from transformation plates were sampled and replicated. These colonies were subjected to colony PCR for positive screening. The colonies were inoculated on a replica plate using a sterile tip and the remaining cells were put in 8$\mu$l sterile water in a PCR tube. The cells were

incubated at 95°C for 8 minutes in a thermocycler. 12$\mu$l reaction mix containing Fermentas Taq DNA polymerase kit 1x buffer, 2,5mM $MgCl_2$, 0,2mM dNTP mix, 0,5u Taq DNA polymerase and 80ng of each P-T primers was added on each tube and the PCR reaction was performed as in Table 2.3.

The PCR products were visualized by ethidium bromide staining after separation by 2% agarose gel electrophoresis using TBE buffer.

Table 2.3: Colony PCR conditions for sequencing

| | | Temperature (°C) | Time |
|---|---|---|---|
| | Denaturation: | 94 | 5 min |
| 25 cycles | Denaturation: | 94 | 30 sec |
| | Annealing: | 58 | 30 sec |
| | Extension: | 72 | 2 min |
| | Final elongation | 72 | 7 min |

### Plasmid isolation

Positive colonies detected by colony PCR were subjected to plasmid isolation for sequencing analysis. 5ml liquid cultures were grown 12-16 hours and 2ml of the cultures of OD 0.6 was used for Qiagen Miniprep plasmid isolation kit(Qiagen, Inc., Valencia, CA). The protocol described in the manufacturer's manualwass performed and the isolated plasmids were eluted in 40$\mu$l EB buffer.

### Ethanol precipitation

The purified plasmids were cleaned up using ethanol precipitation to avoid any interference with sequencing reaction. 0.1 volume of 3M NaOAc (pH 5.2) was added onto the 40$\mu$l plasmid samples and mixed by inverting. 2

volumes of 100% cold ethanol was added and mixed gently. The samples were incubated for 1 hour at -80°C. Plasmids were precipitated by centrifuging for 15 minutes at 13.000rpm at 4°C. The pellets were washed with 70% cold ethanol and air-dried for 10 minutes. The pellets were dissolved in sterile water.

**Sequencing reaction**

For sequencing reaction, 300ng of vector was used as template. 10$\mu$l reaction mix contained 5pmol of each M13 primers and 4$\mu$l of Premix. The PCR reaction was carried out using PTC-100 thermal cycler as shown in Table 2.4.

The PCR products were cleaned up by Ethanol precipitation. 1$\mu$l of 7.5M ammonium acetate and 27.5$\mu$l of 100% cold ethanol was added and mixed. The PCR products were precipitated for 30 minutes by a microcentrifuge at 13.000rpm at 4°C. The pellet was washed with 70% cold ethanol and air dried. The samples were dissolved in 10$\mu$l loading buffer and sequenced.

Table 2.4: Colony PCR conditions for sequencing

| | | Temperature (°C) | Time |
|---|---|---|---|
| | Denaturation: | 94 | 5 min |
| 25 cycles | Denaturation: | 94 | 30 sec |
| | Annealing: | 58 | 30 sec |
| | Extension: | 72 | 2 min |
| | Final elongation | 72 | 7 min |

### 2.2.6 Sequence analysis

The sequences obtained were subjected to VecScreen (NCBI) algorithm in order to elininate the vector sequences. The sequences were compared with

nucleotide and protein sequence databases using BLASTN (EST database) and BLASTX (GenPept database) algorithms (NCBI).

Using ORF finder tool of NCBI, open reading frames of the sequences were detected and the aminoacid sequence of the corresponding protein was obtained.

The protein sequences were searched for known protein motifs using Motif Scan algorithm of SIB - Swiss Institute of Bioinformatics by searching against PROSITE patterns, PROSITE patterns (frequent match producers), PROSITE profiles, Prefile (more profiles), Pfam HMMs (local models), Pfam HMMs (global models) databases (http://myhits.isb-sib.ch/cgi-bin/motif_scan).

For pairwise and multiple alignments, CLUSTALW and CLUSTALX (EBI) algorithms were used.

### 2.2.7 Expression analysis

#### Primer design and PCR amplification

The primers to amplify B1 from the PGEM-T vector and clone to PGFPuv ad PGEX-4T-2 expression vectors were designed with a restriction enzyme site at the 5' end of the forward and reverse primers and additional two arbitrary bases at the 5' ends to increase the restriction efficiency.

The primers to amplify B1 for cloning into PGEX-4T-2 vector has a BAMHI site (GGATCC) on the forward primer and a XHOI site (CTCGAG) on the reverse and the ones for PGFPuv has a SACI site (GAGCTC) on the forward primer and a SPEI site (ACTAGT) on the reverse (Table 2.5).

Amplified PCR product (205bp) was shown in Table 2.6. 50$\mu$ PCR mix contains 30ng template vector PGEMT/B1, 0.5$\mu$M of each primers, 1X reaction buffer, 2.5mM $MgCl_2$, 0.25mM of each dNTPs, and 1 unit Taq DNA

Table 2.5: Primers for B1 to expression vectors

| Primer designation | Sequence (5' -3') | TM(°C) | Size |
|---|---|---|---|
| PGEXB162aaF | GCGGATCCATGGATGCGCA | 62 | 205bp |
| PGEXB162aaR | CGCTCGAGTTAAGATGGCCG | 64 | |
| PGFPuvB173aaF | GCGGATCCATGGACATTCTG | 62 | 205bp |
| PGFPuvB173aaR | CGCTCGAGTTAAGGATACTCC | 60 | |

polymerase. 250bp fragment was extracted from the gel using QiaQuick Gel Extraction kit according to the manufacturer's instructions and eluted from the column with 40$\mu$l EB buffer.

Table 2.6: PCR conditions for amplification of B1 with expression vector primers

| | | Temperature (°C) | Time |
|---|---|---|---|
| | Denaturation: | 94 | 3 min |
| 30 cycles | Denaturation: | 94 | 1 min |
| | Annealing: | 56 | 1 min |
| | Extension: | 72 | 1 min |
| | Final elongation | 72 | 7 min |

**Application of Restriction Enzymes**

PGEX-4T-2 vector and extracted fragment were double digested using BamHI and XhoI restriction enzymes. PGFPuv vector and the corresponding extracted fragment were double digested with SpeI and SacI restriction enzymes. 170ng B1-PGEX-4T-2 fragment, 130ng B1-PGFPuv fragment, 700ng PGEX-4T-2 vector, 500ng PGFPuv vector were double digested with a 20$\mu$l

reaction mix that contains 10 units of each enzymes 1X Multicore Buffer(Promega) and 2$\mu$g BSA. The reaction was performed at 37°C for 4 hours.

### Ligation and transformation

B1 inserts were ligated to the PGEX-4T-2 and PGFPuv vectors in a 15$\mu$l ligation mix that contains 1 unit ligase (Fermentas), 1X reaction buffer (Fermentas), and three different vector insert ratios; 680ng:5600ng, 340ng:2800ng and 170ng:2800ng insert vector amount for PGEX-4T-2 and 520ng:4000ng, 260ng:2000ng and 130ng:2000ng insert vector amounts for PGFPuv. Samples incubated for 2 hours at 22°C and immediately used for transformation.

For transformation, the total 15$\mu$l of ligation mix was put into a sterile micro tube and 50$\mu$l previously prepared and frozen $CaCl_2$ competent Bl21 cells were added onto the ligation mix. The samples were mixed gently and incubated on ice for 20 min. Heat shock step was performed at 42°C for 50 seconds and the samples were put immediately on ice for 2 minutes. 0.5ml prewarmed SOC medium was added and the cells were incubated at 37°C for 1 hour for recovery. 200$\mu$l of the samples were plated on ampicillin/IPTG/X-gal containing LB agar plates and the cells were grown overnight.

White colonies were selected and positive colonies were screened by colony PCR using the primers shown in Table 2.5 as described earlier in Section 2.2.5 with a reaction shown in Table 2.7.

### Total Protein Extract from *E.coli*

5ml liquid cultures of *E.coli* were grown overnight in an ampicillin containing LB broth medium and 10ml starter cultures with $OD_600$ 0.06 was prepared. The expression was induced with 0.75mM IPTG when the $OD_600$ was 0.6. 1 ml aliquotes were taken in every hour, centrifuged at 10.000 rpm for 10 minutes and the pellet was kept at -20°C until use. For the total

Table 2.7: Colony PCR conditions expression vector transformations

| | | Temperature (°C) | Time |
|---|---|---|---|
| | Denaturation: | 94 | 3 min |
| 30 cycles | Denaturation: | 94 | 1 min |
| | Annealing: | 56 | 1 min |
| | Extension: | 72 | 1 min |
| | Final elongation | 72 | 7 min |

extraction the pellets were dissolved in 300$\mu$l lysis buffer containing 50mM Tris-HCl pH:7.5,100mM NaCl, 2.5mM $MgCl_2$, 1m/ml lysozyme and protease inhibitors. The samples were incubated on ice for 40 minutes and centrifuged at 13.000 rpm for 15 minutes at 4°C. The supernatant was containing the soluble protein fraction. The pellet, containing the insoluable protein fraction was dissolved in 300$\mu$l lysis buffer and both kept at -20°C until its use.

**SDS-PAGE**

5ml of 12% SDS resolving gel was prepared with 625$\mu$l 3M Tris-HCl pH:8.9, 2ml 30% Acrylamide, 25$\mu$l 20% SDS, 37.5$\mu$l 10% APS and 2.5$\mu$l TEMED. 2.5ml of 5% SDS stacking gel was prepared with 125$\mu$l 1M Tris-HCl pH:6.8, 425$\mu$l 30% Acrylamide, 12.5$\mu$l 20% SDS, 10% APS and 2.5$\mu$l TEMED. The gels were polymerized overnight at 4°C and run with 20mA for about an hour.

**Native-PAGE**

5ml of 8% native resolving gel was prepared with 625$\mu$l 3M Tris-HCl pH:8.9, 1.333ml 30% Acrylamide, 37.5$\mu$l 10% APS and 2.5$\mu$l TEMED. 2.5ml 5%native stacking gel was prepared with 125$\mu$l 1M Tris-HCl pH:6.8, 425$\mu$l 30%

Acrylamide, 10% APS and 2.5$\mu$l TEMED. The gels were polymerized overnight at 4°C and run with 20mA for about an hour.

### 2.2.8 Real-time PCR

For Real-Time PCR analysis, 18S ribosomal RNA was used as an housekeeping gene and the primers were designed as in Table 2.8. The concentration and annealing temperatures of all primers were optimized prior to the reaction. For a 25 $\mu$l PCR, 500ng first strand cDNA of Zn– and MS plants were used as template. 0.5 $\mu$M final concentration of each primer and 1X of SYBR Green were used. The amplifications were performed in Biorad iCyclerQ as shown in Table 2.9.

Table 2.8: Primers used for Realtime PCR

| Primer designation | Sequence (5' - 3') | Amplicon |
|---|---|---|
| 18SribosomalRNA For | ATG ATA ACT CGA CGG ATC GC | 200 bp |
| 18SribosomalRNA Rev | CTT GGA TGT GGT AGC CGT TT | |
| B1 For | GGG ATG GTC TGA TCT GGG G | 309 bp |
| B1 Rev | GAC ACC GCC TGA AGC ATC G | |

### 2.2.9 RACE:Rapid amplification of cDNA ends

The full length mRNA of the first identified fragment (415bp) amlified with P3-T1 primers in Creeping bentgrass in the tissue culture trial was obtained using The GeneRacer Kit of Invitrogen.

#### Primer design

Two nested gene specific primers for both 3' and 5' RACE were designed to use together with the two nested primers supplied with the kit.(Table 2.10)

Table 2.9: Real Time PCR conditions

| | | Temperature (°C) | Time |
|---|---|---|---|
| Cycles | Denaturation: | 94 | 15 min |
| 40 | Denaturation: | 94 | 30 sec |
| | Annealing: | 56 | 30 sec |
| | Extension: | 72 | 1 min |
| | Final elongation | 72 | 10 min |
| 80 | Melting: | 53+(0.5/cycle) | 10 sec |

Table 2.10: Primers designed for RACE and the primers supplied with GeneRacer Kit

| Primer designation | Sequence (5' -3') | TM(°C) |
|---|---|---|
| GeneRacer5' | CGACTGGAGCACGAGGACACTGA | 74 |
| GeneRacer5'nested | GGACACTGACATGGACTGAAGGAGTA | 74 |
| GeneRacer3' | GCTGTCAACGATACGCTACGTAACG | 74 |
| GeneRacer3'nested | CGCTACGTAACGGCATGACAGTG | 72 |
| Genespecific5' | ATTCGCACCATCGCTGTCAA | 65 |
| Genespecific5'nested | ATTCGCACCATCGCTGTCAA | 65 |
| Genespecific3' | CGACTCGGAAAGCTGCTTGA | 66 |
| Genespecific3'nested | CATGGTGTCGGTGGTGCTTG | 66 |

**RACE PCR**

1$\mu$g of total RNA was subjected to dephosphorylation and mRNA cap structure removal steps and the product was ligated with the RNA oligo provided and subjected to reverse transcription according to the manufacturer's instructions.

The cDNA ends applified with PCR using the combinations of inner and outer primers and negative controls for each primer according to the program was shown in Table 2.11 using a hot start by the addition of enzyme later. For 50 $\mu$l PCR, 0.5$\mu$l of the obtained cDNA was used as template. The PCR mix contained 3$\mu$l of 10$\mu$M race primers and 2$\mu$l of 10$\mu$M of gene specific primers, 1X reaction bufer, 0.2mM dNTPs, 0.5 unit Taq polymerase and 2.5mM $MgCl_2$.

Table 2.11: Race PCR

| | | Temperature (°C) | Time |
|---|---|---|---|
| 5 cycles | Heating Lid | 95 | hold |
| | Denaturation | 94 | 30 sec |
| | Extension | 72 | 1 min |
| 5 cycles | Denaturation | 94 | 30 sec |
| | Extension | 70 | 1 min |
| 25 cycles | Denaturation | 94 | 30 sec |
| | Annealing | 60 | 30 sec |
| | Extension | 72 | 1 min |
| | Final elongation | 72 | 10 min |

# Chapter 3

# Results

## 3.1 Green house trial: Shoot growth and zinc concentrations

### 3.1.1 Zinc concentration of seeds

The concentration and content of zinc in the seeds were measured before starting the green house trial (Table 3.1). The results indicated that Colonial and Creeping bentgrass almost had the same zinc content per seed whereas Velvet bentgrass had a higher zinc content per seed. Due to its higher amount of zinc in the seed, Velvet bentgrass was expected to have a higher tolerance to zinc deficiency than the other two genotypes.

Table 3.1: Seed ICP results

| Grass | Seed Zn content | Seed Zn concentration |
|---|---|---|
| Colonial bentgrass | 2.74($\mu$g/seed) | 47(mg/kg) |
| Creeping bentgrass | 2.78($\mu$g/seed) | 36(mg/kg) |
| Velvet bentgrass | 3.85($\mu$g/seed) | 66(mg/kg) |

### 3.1.2 Dry weight

The shoot dry weight of plants per pot for three parallels were measured for Creeping, Colonial and Velvet bentgrass after four weeks of growth under three different zinc concentrations and from the data the total dry weight per plant was calculated (Figure 3.1). The dry weight per plant increased in response to zinc supply in all genotypes tested.

The growth of Creeping bentgrass decreased by 67% when there was no zinc supply and by 35% when 0.1ppm zinc was supplied compared to 5ppm of zinc supply. The growth of Colonial bentgrass decreased by 87% when there was no zinc supply and by 74% when 0.1ppm zinc was supplied when compared to 5ppm of zinc supply. The growth of Velvet bentgrass decreased by 88% when there was no zinc supply and by 87% when 0.1ppm zinc was supplied compared to 5ppm of zinc supply. These results indicated that the most tolerant species to zinc deficiency in terms of dry weight was Creeping bentgrass as growing significantly more than the other species under the same conditions. The growth of Velvet bentgrass was affected slightly more than Colonial bentgrass; however, it was quite unresponsive to 0.1ppm zinc application whereas Colonial bentgrass was responsive.

It can be concluded that, in terms of dry weight, the most zinc deficiency tolerant species was Creeping bentgrass whereas the most susceptible one was Velvet bentgrass.

### 3.1.3 Zinc concentration and content

The results for concentration of zinc from the element analysis of Creeping, Colonial and Velvet bentgrass after four weeks of growth under three different zinc concentration were shown in Figure 3.2. The data for zinc and other elements (Ca, Al, Cu, K, Mg, Mn, P, S, Zn, Fe) can be found in Appendix

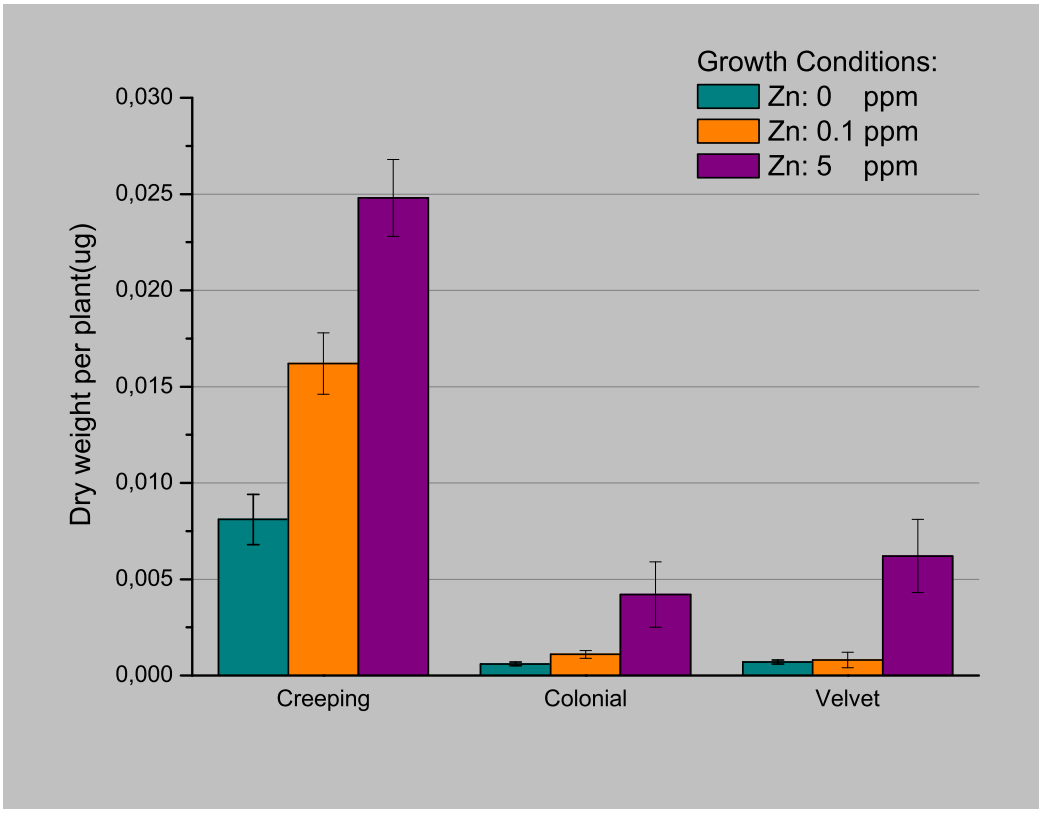


Figure 3.1: Dry weight per plant in response to different zinc concentrations after four weeks of growth for Creeping, Colonial and Velvet bentgrass obtained from three parallels

A.3.

The data verified that the zinc concentration in the shoots increased as the applied zinc level was increased during the growth . The unexpected amount of zinc concentration in Colonial bentgrass grown without Zn was probably due to soil contamination during harvesting. The small variations in the graph can be explained with the total dry weight of plants and the content of zinc per plant can be seen in the Figure 3.3.

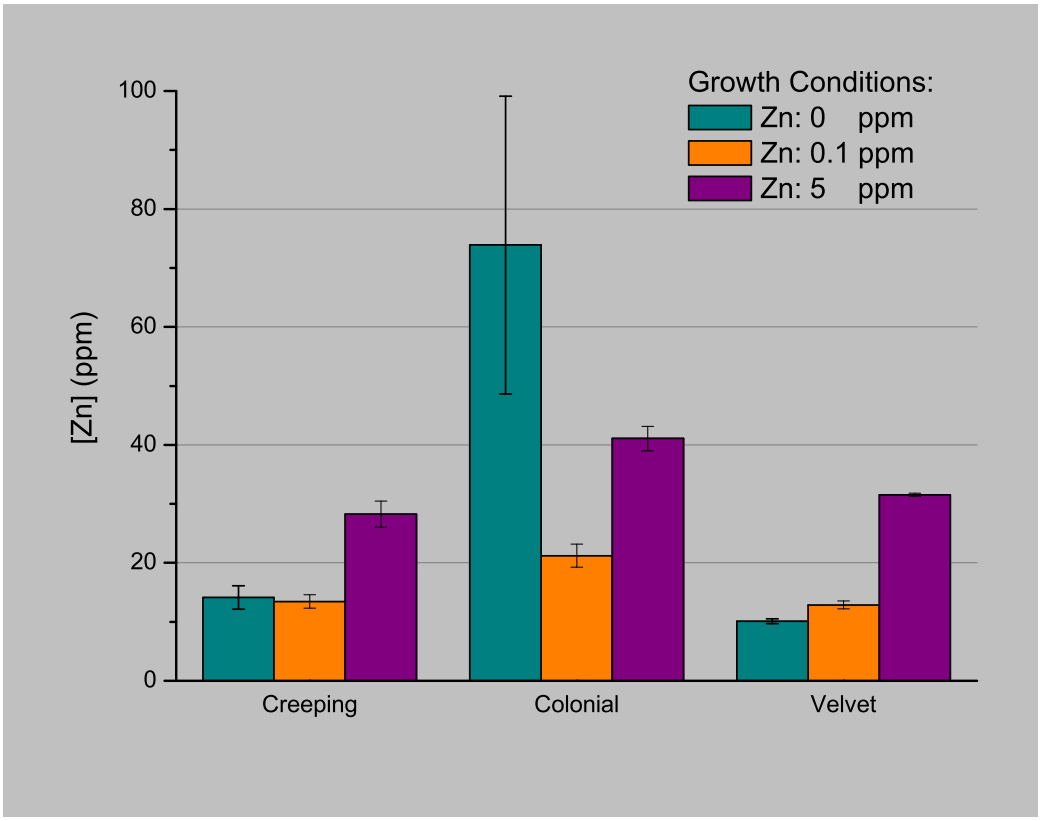


Figure 3.2: Zinc concentration in plants in response to different zinc concentrations after four weeks of growth for Creeping, Colonial and Velvet bentgrass obtained from three parallels

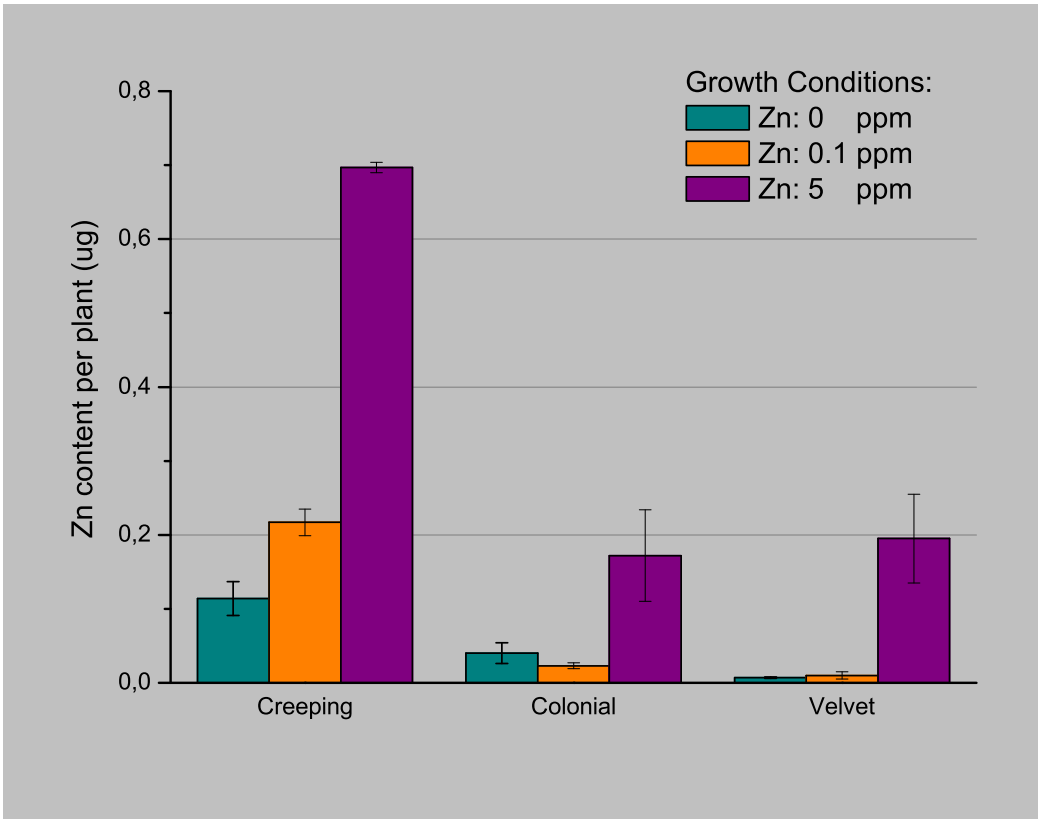


Figure 3.3: Zinc contents of plants in response to different zinc concentrations after four weeks of growth for Creeping, Colonial and Velvet bentgrass obtained from three parallels

## 3.2 mRNA differential display of Creeping bentgrass grown in sterile tissue culture

Total RNAs from the plants grown in 0 and 5ppm zinc concentrations were subjected to DNAs treatment and used as a template for differential display analysis to identify differentially expressed genes in response to the zinc concentration. Total cDNAs were amplified with 72 primer combinations (Table 2.1).

Several fragments in varying sizes ranged from 100bp to 2000bp were obtained for each primer combination. Four differentially amplified fragments that showed a significant difference between zinc deficient plants and the plants grown under 5ppm zinc concentration were selected and extracted from the gel. The electrophoresis result of the differential display PCR results amplified with P1-T7(a), P3-T1(b), P4-T2(c) and P6-T5(d) primers was shown in Figure 3.4. The extracted fragments of 200bp, 500bp, 200bp and 200bp respectively were shown with the arrows . The fragments of interests were extracted from the gel, cloned to PGEM-T easy sequencing vector. The vector was amplified in *E.coli* host cells, isolated and sequenced for futher analysis. The sequences of the four fragments obtained from the mRNADD application were depicted in Table 3.2.

### 3.2.1 BLASTX algorithm was used to identify the similarity of the obtained sequences with the known proteins

The sequences were analyzed for their similarity to the known proteins using BLASTX algorithm. The BLASTX results indicated similarity to many different proteins identified in various organisms such as the proteins that were shown in Table 3.3.

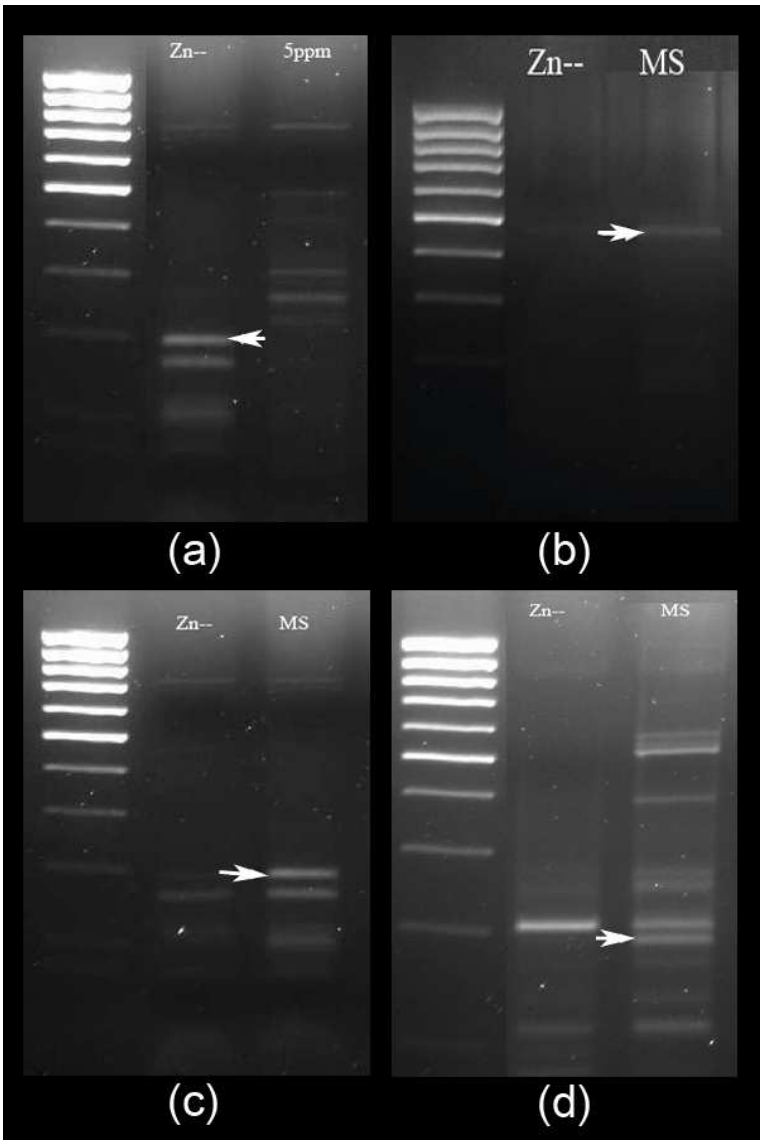


Figure 3.4: mRNADD results of 50$\mu$l PCR products of creeping bentgrass tissue culture trial prior to gel extraction for sequencing. Zn– in all gel pictures refers to the plants grown under zinc deficiency and MS refers to the ones grown under 5ppm Zn. GeneRuler100bp DNA marker was used in all gels. (a)PCR products of P1T7 primers. The 156bp band shown with an arrow was extracted from the gel. (b)PCR products of P3T1 primers. The 415bp band shown with an arrow was extracted from the gel. (c)PCR products of P4T2 primers. The 199bp band shown with an arrow was extracted from the gel. (d)PCR products of P6T5 primers. The 175bp band shown with an arrow was extracted from the gel.

Table 3.2: Sequences of the isolated four fragments from Creeping bentgrass of tissue culture trial

| Primers | Size(bp) | Sequence |
|---|---|---|
| P1-T7 | 156 | GCT CTG AGT AAG AGA CTG AGA TAA AGA TAT CAA AAG ATT CAA GCA TCA CAG TTA TAC CAA AAT TAA TCT TAT TCC AGG ACA AGC ATG TTA CAC TAA GAA TGA CAG CGG TGC TTT CAA GAG GGT GCT CAA AAA AAA AGA TAT CAC TCA GCA TAA TGA |
| P3-T1 | 415 | AAA GAC CGC CGC CTC CCC GGC GCA CGA CAT GGA CAT TCT GAT CTA TGG TCG GTG GCT CAC GAG GAG GGT GCA CAA CAC ATA CAC ATG GAT GCG CAC ACA ACT GGA GGA CAA CTA TAC TCA CAT GGT GCT ATA CTG GTC TGT GCA GGC TCA CAG TTG GAG GCA GTA CCT ACA ATC AAT TCG CAT ACG TCA GTA CTA TCG GTT CTT ACG CTG TTG GAA TCG GTG CAT TCA GTT ATC ATT GGA GTA TCC TTA AGT GCA TCT GTA CGG CCA TCT TAA GCC AAT CAG GTG CCC TAC TTG CTC AAC CAG CTT CCG TCA GGT CTT TAT GTG TGG ACG TTT GGT TTG CAT TGT CAG TTA CGC TAC TTG GAA CCT ACG GGC GTC ATT GTT TCC TTA AAA AAA AAG ATA TCA CTC AGC ATA ATG A |
| P4-T2 | 199 | AAT AAG GAT AGA GAG GTT GCT GTT AGA TGT AGT AAT AGA AGA CAT ATT TAT CAA TGT ACT GAA ACA AAA AAA TCT AAA TAT AAT ACC CTT GAG GGG TTC CTC CTT GAA GTG TTG CAT TGT TAT TTA ATG GTT TCT AGG AGT ATG GAG AAA ATG TTT GCC CTC TAA TTG GTA AAA AAA AAG ATA TCA CTC AGC ATA ATG A |
| P6-T5 | 175 | GGC GAG GGA AGA ACT GCT GAA GAT ATA AGT ANA AGC CCA CCC CAA GAT GAG TGC TTT CTC CTC CGA CTT CCC TAG AGC CTA CGG TGT CAC AGC CGA AAC AGC GAC GGG TTC TCC ACC CAT ATG GGG ATG GAG CGA CAG AAG TAT GGA AAA AAA AAG ATA TCA CTC AGC ATA ATG A |

According to these results, the fragment that was amplified with P4-T2 primers did not show any significant similarity to known proteins in GeneBank database. On the other hand, the band amplified with P1-T7 primers showed 44% similarity to a protein identified in Chlorobium ferrooxidans DSM 13031 strain which was a phototrophic bacterium that was enriched with feroous iron (Table 3.3). The protein was identified upon the enrichement of iron and that might be important in metal related mechanisms besides it was found to be conserved for bacterial and plant plasmids.

The fragment amplified with P3-T1 showed similarity to many known proteins some of which were more interesting (Table 3.3). It showed 52% identity to a zinc transporter of *Oryza sativa* from the ZIP3 zinc transporter family. In the same frame, it also showed 47% identity to an hypthetical protein in *Oryza sativa* thatwass found to be in ZIP zinc transporter family. Also, it had a 47% identity with another zinc transporter ZIP isolated from *Triticum aestivum*. Due to these significant similarities, the fragment was thought to be a candidate ZIP transporter identified in Creeping bentgrass.

The fragment amplified with P4-T2 primers showed 100% similarity with a putative casein kinase I of *Dendrobium grex Madame Thong-In* that was characterized as a differentially expressed gene during orchid floral transiton (Table 3.3).

The fragment amplified with P6-T5 primers showed 100% similarity with a putative polyprotein in *Oryza sativa* (Table 3.3). It also showed similarity to HtaA-like surface protein of *Propionibacterium acnes*. HtaA domain is found in secreted proteins implicated in iron acquisition and transport (pfam04213). The fragment had 46% similarity to a hypothetical protein of *Aspergillus niger* that is similar to metal homeostasis protein Bsd2 in *Saccharomyces cerevisiae*. It also showed 48% similarity to the large sub-

unit of F420-nonreducing hydrogenase II of *Methanosarcina barkeri* which is a Ni,Fe-hydrogenase involved in energy production and conversion. It was 50% similar to CG5591-PA protein of *Drosophila melanogaster* which has a PHD-finger region that folds into an interleaved type of Zn-finger chelating two Zn ions. Moreover, it showed 57% similarity to a ferrochelatase identified in *Polaromonas naphthalenivorans* that catalyzes the insertion of ferrous iron into the protoporphyrin IX ring yielding protoheme.

BLASTX results indicated that the fragments identified in this study were important transcripts due their similarity to different proteins that were related to metal ion involving pathways. This result clearly indicated that mRNADD tool worked perfectly to identify Zn responsive genes. The obtained transcripts can readily be located on molecular linkage maps to identify chromosomal location of Zn responsive genes in grass genome.

### 3.2.2 ORF regions of the obtained sequences

The open reading frames of the four sequences were detected using ORF Finder algorithm of NCBI. The first fragment amplified with P1-T7 primers and the third fragment amplified with P4-T2 primers did not have a ORF region where as the second fragment that was amplified with P3-T1 primers, had three ORFs of 73,62 and 59 amino acids long in the frames 2,1 and -3, respectively (Table 3.4). The last fragment amplified with P6-T5 primers had two ORF regions which are length 41 and 27 amino acids long in the frames 2 and -3, respectively (Table 3.4).

### 3.2.3 Real-time PCR for the fragment amplified with P3-T1 primers in Creeping bentgrass

Real time PCR was performed using SYBR Green to compare the expression level of the fragment obtained with P3-T1 primers from Creeping bentgrass

Table 3.3: BLASTX results of the isolated four fragments in tissue culture trial using NCBI BLASTX algorithm with Blossom80 and PAM30 matrices

| Primers | BLASTX hit | Identity | Frame |
|---|---|---|---|
| P1-T7 | gi:110598354 conserved hypothetical protein [Chlorobium ferrooxidans DSM 13031] | 44% | +3 |
| P3-T1 | gb:AAP85537.1 zinc transporter ZIP3 [Oryza sativa (japonica cultivar-group)] | 52% | +1 |
| | gb:EAY95519.1 hypothetical protein OsI016752 [Oryza sativa (indica cultivar-group)] | 47% | +1 |
| | gb:AAW68439.1 zinc transporter ZIP [Triticum aestivum] | 47% | +1 |
| P4-T2 | gb:AAD20819.1 putative casein kinase I [Dendrobium grex Madame Thong-In] | 100% | -3 |
| P6-T5 | gb:AAU43927.1 putative polyprotein [Oryza sativa (japonica cultivar-group)] | 43% | +2 |
| | gb:ABF13594.1 HtaA-like surface protein [Propionibacterium acnes] | 40% | +3 |
| | ref:XP001390958.1 hypothetical protein An06g01360 [Aspergillus niger] | 46% | +3 |
| | ref:YP305367.1 F420-nonreducing hydrogenase II, large subunit [Methanosarcina barkeri str. fusaro] | 48% | +3 |
| | ref:NP611847.2 CG5591-PA [Drosophila melanogaster] | 50% | -1 |
| | ref:YP983193.1 Ferrochelatase [Polaromonas naphthalenivorans CJ2] | 57% | -2 |

Table 3.4: ORFs in the isolated four sequences

| Primers | Frame | Sequence | Length(aa) |
|---|---|---|---|
| P1-T7 | 1 | Met L H Stop | 3 |
| | -2 | Met L V L E Stop | 5 |
| P3-T1 | 1 | Met D A H T T G G Q L Y S H G A I L V C A G S Q L E A V P T I N S H T S V L S V L T L L E S V H S V I I G V S L S A S V R P S Stop | 62 |
| | 2 | Met D I L I Y G R W L T R R V H N T Y T W Met R T Q L E D N Y T H Met V L Y W S V Q A H S W R Q Y L Q S I R I R Q Y Y R F L R C W N R C I Q L S L E Y P Stop | 73 |
| | -3 | Met I T E C T D S N S V R T D S T D V C E L I V G T A S N C E P A Q T S I A P C E Y S C P P V V C A S Met C Met C C A P S S Stop | 59 |
| | -2 | Met Q Q H L Q K G P Q D K Stop | 12 |
| | -3 | Met L S D I F F F K E T C V L V Y Stop | 16 |
| P4-T2 | 1 | Met V S R S Met E K Met F A L Stop | 12 |
| | 3 | Met Y Stop | 2 |
| | -3 | Met L S D I F F F T N Stop | 10 |
| P6-T5 | 2 | Met S A F S S D F P R A Y G V T A E T A T G S P P I W G W S D R S Met E K K R Y H S A Stop | 41 |
| | -2 | Met G G E P V A V S A V T P Stop | 13 |
| | -3 | Met L S D I F F F P Y F C R S I P I W V E N P S L F R L Stop | 27 |

grown in tissue culture in response to different zinc supply (Figure 3.1). 18S ribosomal RNA was used as a reference gene and the CT value of the reference gene was equalized for both plants that were grown with (5ppm)and without zinc treatment. The PCR conditions were optimized for the primers and initial template.

The CT value for the fragment (named B1) was then measured 24.7 for Zn 5 ppm and 29.8 for without Zn indicating that there was $2^5$ fold of difference between the initial amount of the transcript of interest for 5ppm and without zinc growth conditions when normalized according to the reference gene (Figure 3.5A).

To evaluate whether specific PCR products were the source of the florescence, the melt curve of each sample was measured at the end of the program. The samples gave a pick at the specific melting temperatures of the double stranded amplicons (Figure 3.5B).

The standart curve of the CT values of the serial dilutions of initial template amount was shown in Figure 3.6, indicating that there was a linear correlation between the CT values and the base logarithm of initial template amount. This means that the florescence was significant in the range of the serial dilutions from 500ng to 31.25ng.

To compare the expression levels, the real-time PCR was also done with the cDNAs obtained from the plants grown in green house with 5ppm zinc and without zinc. The results indicated that there was a high correlation between the tissue culture and green house trial results with a slight increase in the difference. The CT value for the fragment (named B1) was then measured 23.7 for 5ppm Zn and 29.6 for without Zn indicating that there was $2^6$ fold of difference between the initial amount of the transcript of interest for 5ppm and without zinc treatment when normalized according to the reference

gene(Figure 3.7A). The melting curve graph supports that the florescence was specific to amplicons of interest (Figure 3.7B) and the standard curve of the dilutions of the template proved that the amount of template was in the significance range of florescence (Figure 3.8).

The real-time PCR results indicated the the expression level of the transcript is down-regulated $2^5$-$2^6$ fold in response to zinc deficiency.

### 3.2.4 Expression of the ORF regions of the fragment amplified with P3-T1 primers

The fragment that was amplified with P3-T1 primers in Creeping bentgrass had very significant similarity with the known ZIP zinc transporters and had two ORF regions. The two ORF regions were cloned to PGEX-4T-2 expression vector and expressed as a GST fused protein in *E. coli*. However, the results indicated that both of the ORF products were being degraded either in the cell or during the isolation process. In (Figure 3.9A,B) although the control vector expressing only GST was clearly visible in the expected size (26kDa), the GST fused protein (expected to be 32kDA) was seen only 27-28kDa. In the native gel picture, although the control vector expressing GST only showed an intact band, the GST fused protein did not give an intact band (Figure 3.9C). Therefore, it is assumed that the the protein products of the ORF regions were not stable.

### 3.2.5 RACE for the fragment amplified with P3-T1 primers

The differentially expressed fragment, amplified with P3-T1 primers, was found to be candidate ZIP zinc transporter of Creeping bentgrass (Table 3.3). 5' and 3' RACE was performed to obtain the full length mRNA sequence of the fragment. The fragments amplified in the RACE PCR that were different

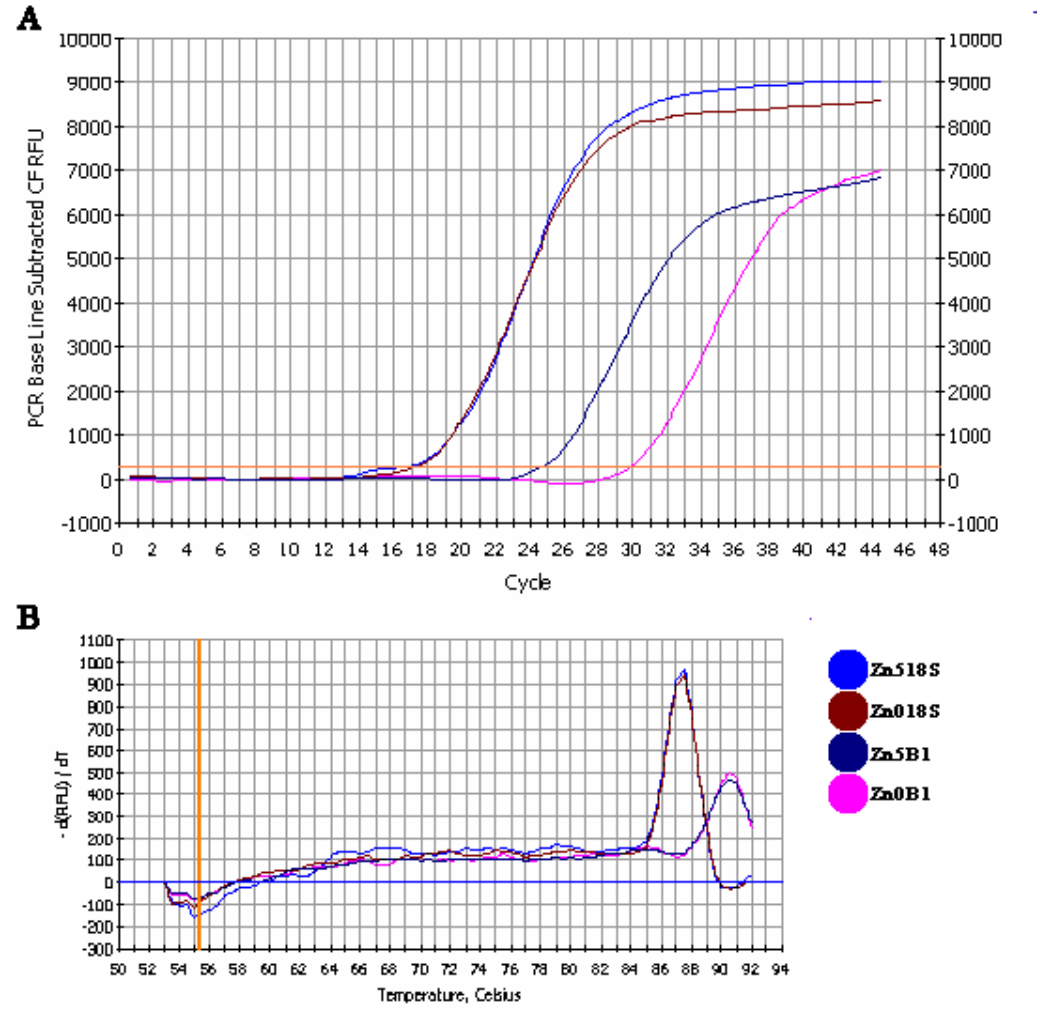


Figure 3.5: Real-time amplification plots of the fragment amplified with P3-T1 primers in Creeping bentgrass grown in tissue culture. 18S ribosomal RNA was used as a reference gene. (A)The PCR Base Line Subtracted Curve Fit Data with calculated threshold using the maximum curvature approach is 266.9,per-well baseline cycles have been determined automatically, data analysis window is set at 95.00% of a cycle, centered at end of the cycle, weighted mean digital filtering being applied and global filtering is off. (B)The melt curve with weighted mean digital filtering applied, global filtering is off and threshold for automatic peak detection is set at 1.00.

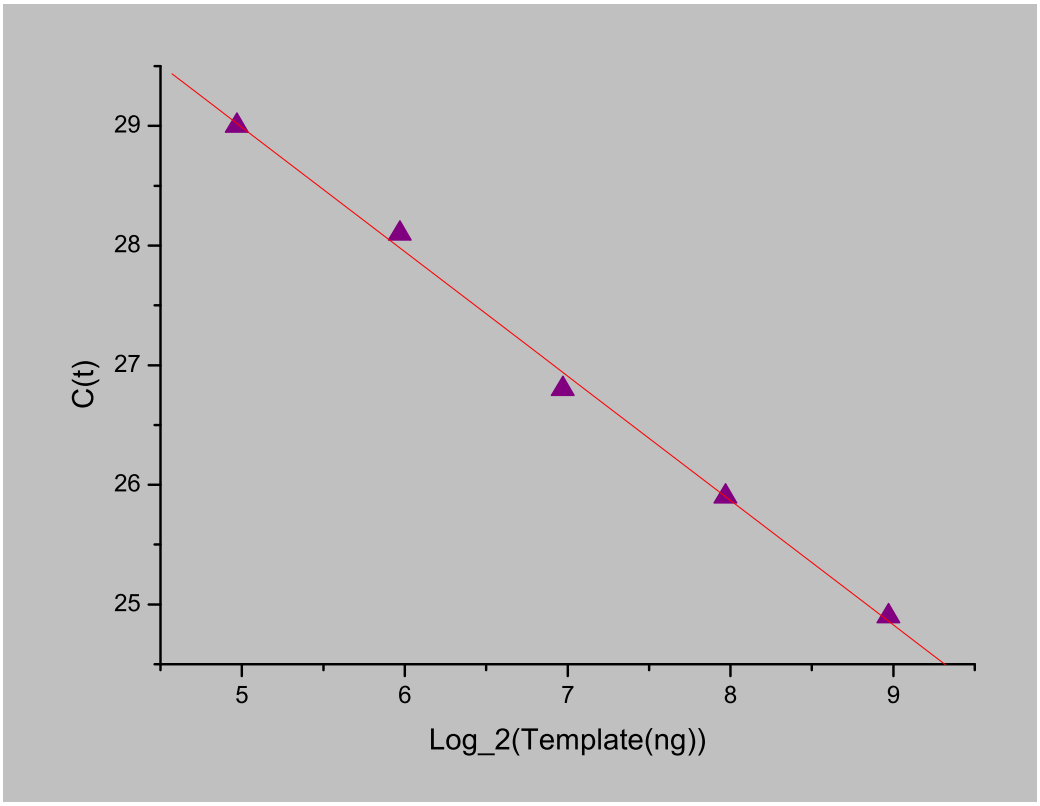


Figure 3.6: Real Time PCR standard curve for tissue culture trial: Amplification standard curve with linear correlation between the cycle threshold (CT) and the base two logarithm of initial amount of cDNA template ranging from 500ng to 31.25ng of cDNA.

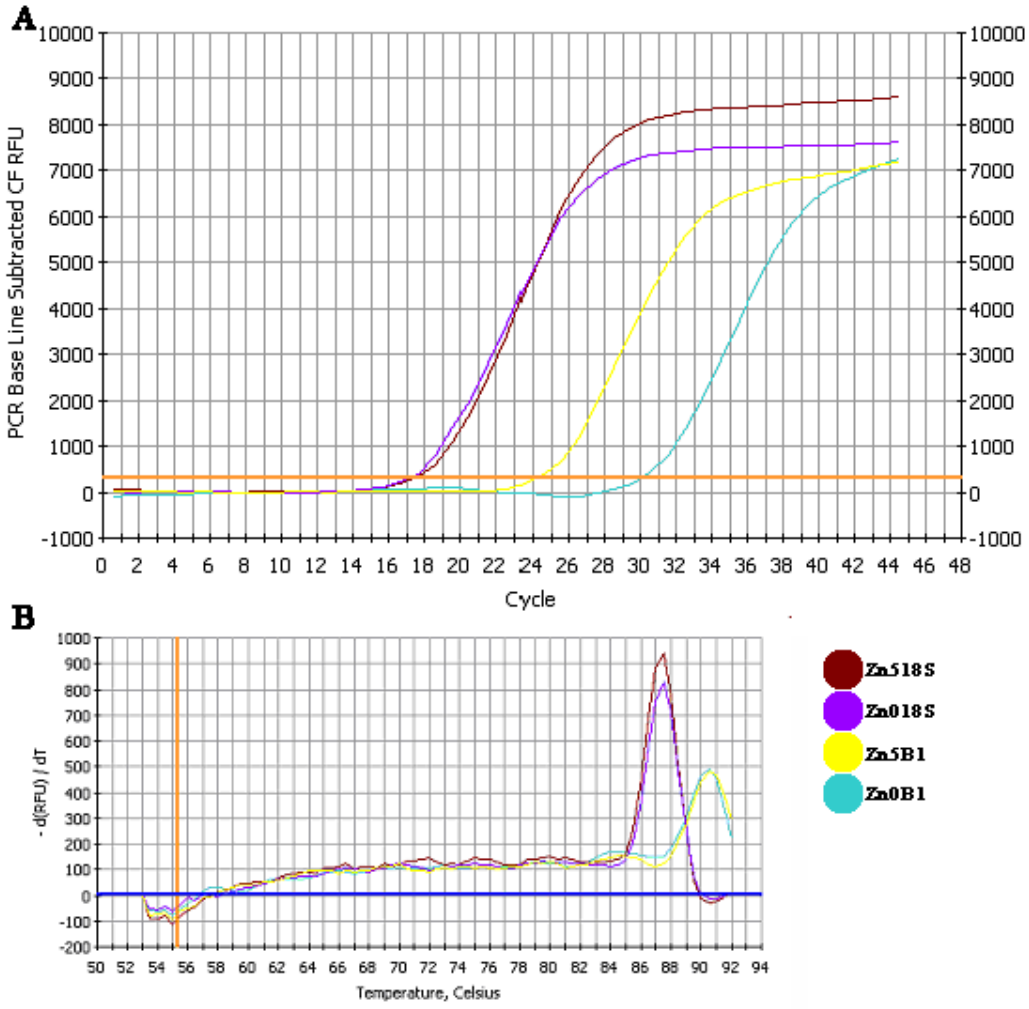


Figure 3.7: Real-time amplification plots of the fragment amplified with P3-T1 primers in Creeping bentgrass grown in green house. 18S ribosomal RNA was used as a reference gene. (A)The PCR Base Line Subtracted Curve Fit Data with calculated threshold using the maximum curvature approach is 266.9,per-well baseline cycles have been determined automatically, data analysis window is set at 95.00% of a cycle, centered at end of the cycle, weighted mean digital filtering being applied and global filtering is off. (B)The melt curve with weighted mean digital filtering applied, global filtering is off and threshold for automatic peak detection is set at 1.00.

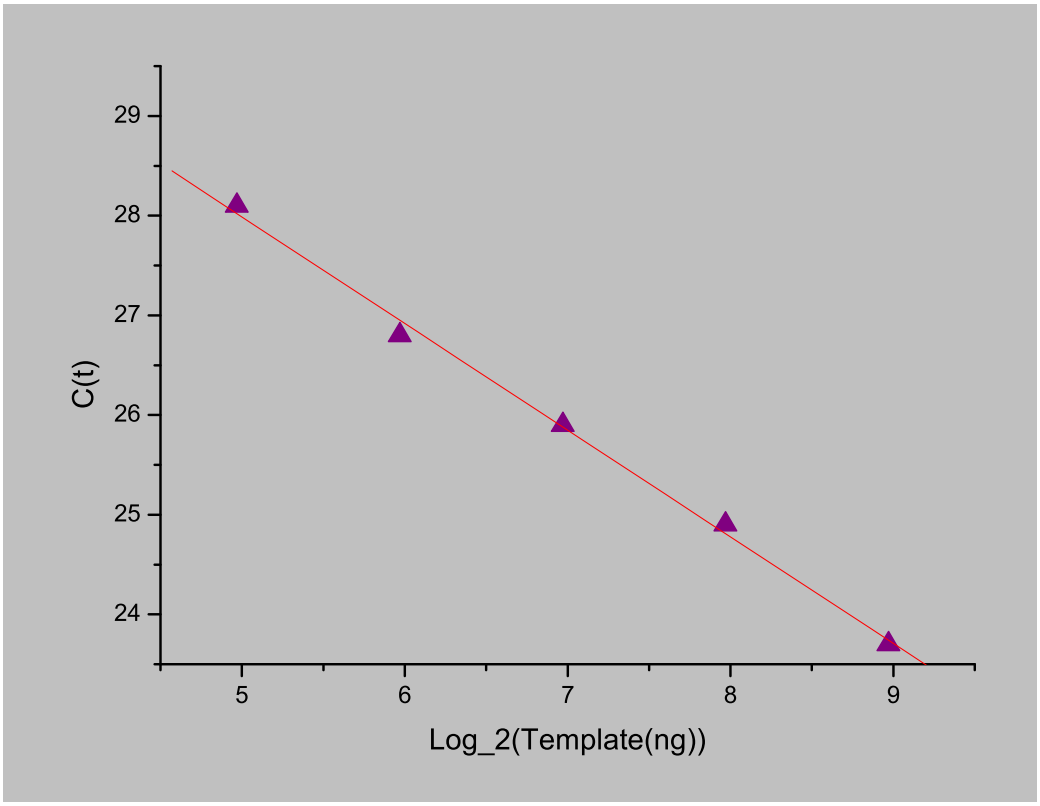


Figure 3.8: Real Time PCR standard curve for green house trial: Amplification standard curve with linear correlation between the cycle threshold (CT) and the base two logarithm of initial amount of cDNA template ranging from 500ng to 31.25ng of cDNA.

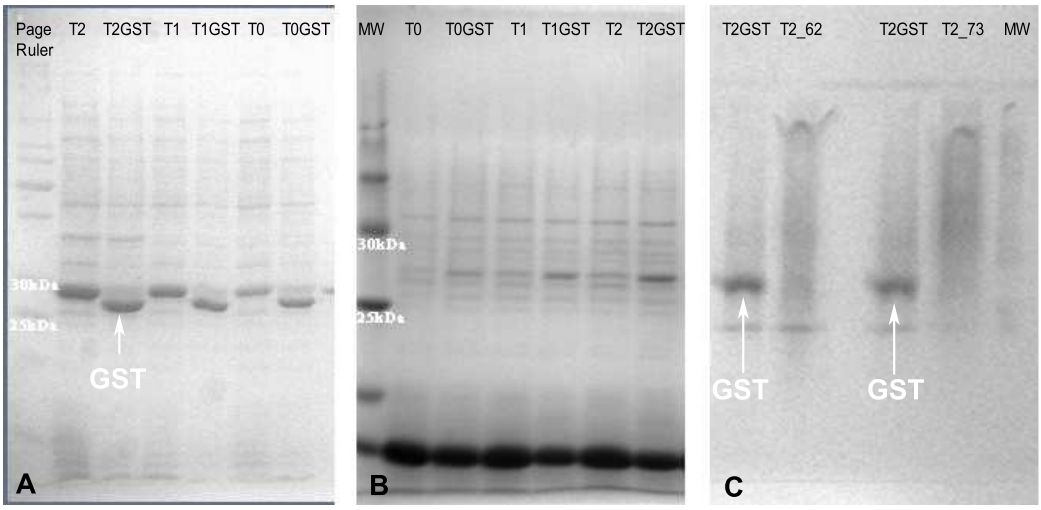


Figure 3.9: SDS and native PAGE results of the 62 and 73 aminoecid ORF regions. (A) SDS PAGE of 73aa ORF from one to three hours after induction (B) SDS PAGE of 62aa ORF from one to three hours after induction (C) NATIVE PAGE of 62 and 73aa ORF regions at three hours after induction

from the negative controls were extracted from the gel and sequenced. The full mRNA sequence was found to be 1009bp in length, having 495bp in the 5' end and 99bp in the 3' end of the fragment previously obtained (Table 3.5).

Previously obtained fragment was analyzed for its similarity with the known protein sequences using BLASTX algorithm with BLOSSOM62. The results indicated that the sequence obtained was ZIP family zinc transporter because it showed high level of similarities with many ZIP zinc transporters from various organisms (Table 3.6). The protein product was highly similar *Oryza sativa* ZIP proteins (gb:AAP85537.1). BLASTN and tBLASTX algorithms also gave similar results with ZIP transporter coding ESTs.

The open reading frame of the full length mRNA sequence was detected using ORF Finder algorithm of NCBI. According to the results, the mRNA had 238 amino acid ORF in frame 1(Table 3.7). According to the PFAM data, the average length of the known ZIP family proteins is about 270 amino acids

which was not significantly different from the size of the detected ORF.

This is the first isolated ZIP zinc transporter in Creeping bentgrass.

### 3.2.6 Phylogenetic analysis of ZIP family proteins

The ORF region detected in the full length mRNA sequence was subjected to multiple alignment with the known plant ZIP family proteins using CLUSTALX algorithm. Figure 3.10 clearly indicated that the protein product obtained was higly conserved with the known plant ZIP family proteins. Cladogram analysis indicated that the protein was mostly similar to ZIP zinc transporters of *Oryza sativa*(GI47169687) and *Triticum aestivum* (GI58221593) as it was also found in BLASTX searches (Figure 3.11).

Figure 3.12 showed the pairwise alignmet results of the protein product of the full mRNA sequence with its highest BLASTX hit *Oryza sativa* zinc transporter ZIP3(gb:AAP85537.1). According to the alignment results, although the ZIP3 was longer than the product, they were highly conserved in the overlapping regions.

## 3.3 Application of mRNA differential display to Agrostis species grown in green house

The total cDNAs obtained from Colonial,Creeping and Velvet bentgrass species were subjected to mRNA differential display method with 72 different primer combinations (Section 2.2.4,Table 2.1).

The gel electrophoresis results of the fragments isolated from Colonial bentgrass were shown in Figure 3.13. The differentially expressed fragments were extracted from the gel and sequenced. The sequences of the the fragments obtained by cloning the fragments to PGEM-T easy vector were shown in Table 3.8. P6T3 primer pair amplified a fragment size of 128bp that was

Table 3.5: The full mRNA sequence of the fragment amplified with P3-T1 primers obtained by RACE

| Primers | Size(bp) | Sequence |
|---|---|---|
| P3-T1 | 1009 | CCG CGC GAC CGT CAG CGA ATT ACG GGC AAT CAA TCC ACA TAC TCA ACA ATT ATG GGA GCC AAG AAG CAT ACC TTG CAA GTG CTT CCA TGG CTA CTG CTC TTT GCG CAG CAC ACT GCA GCC AGT GCC TGC GAC TGT GCT AAC ACC ACA GAC GGG GCA GAC AGA CAG GGT GCA ATG AAG CTA AAG CTC ATT GCC ATT GCA TCC ATC CTT GCA GCT GGG GCG GCT GGT GTC TTG GTG CCA GTG ATT GGC CGC TCC ATG GCT GCG CTG CGC CCT GAT GGT GAC ATC TTC TTT GCT GTC AAG GCA TTT GCA GCC GGC GTC ATC CTT GCC ACT GGC ATG GTG CAC ATT CTT CCA GCG GCG TTT GAT GCG CTC ACA TCT CCA TGC CTC AAA AGG GGT GGT GGG GAT AGG AAT CCC TTC CCC TTT GCG GGC CTC AGA CTC GCT GGC TGC TGG GTA CTA CCG CCG GTC TCA CTT GTG GTG GGG ATA GGA ATC CCT TCC CCT TTG AAA GAC CGC CGC CTC CCC GGC GCA CGA CAT GGA CAT TCT GAT CTA TGG TCG GTG GCT CAC GAG GAG GGT GCA CAA CAC ATA CAC ATG GAT GCG CAC ACA ACT GGA GGA CAA CTA TAC TCA CAT GGT GCT ATA CTG GTC TGT GCA GGC TCA CAG TTG GAG GCA GTA CCT ACA ATC AAT TCG CAT ACG TCA GTA CTA TCG GTT CTT ACG CTG TTG GAA TCG GTG CAT TCA GTT ATC ATT GGA GTA TCC TTA AGT GCA TCT GTA CGG CCA TCT TAA GCC AAT CAG GTG CCC TAC TTG CTC AAC CAG CTT CCG TCA GGT CTT TAT GTG TGG ACG TTT GGT TTG CAT TGT CAG TTA CGC TAC TTG GAA CCT ACG GGC GTC ATT GTT TCC TTA AAA AAA AAG ATA TCA CTC AGC ATA ATG ACT AGA TTT TCT AAA ACC AAA GCT TAT CTC AGG TGA TCT CTT TGT ACT TTA TGA TAT GAT AAT ACA TGA TGA CTT AAC TTG TTC TTA AAA AAA AAA AAA A |

Table 3.6: BlastX results of the full mRNA sequence using NCBI BLASTX algorithm with Blossom62 matrix

| BLASTX hit | Identity | Frame |
|---|---|---|
| gb:AAP85537.1 zinc transporter ZIP3 [Oryza sativa (japonica cultivar-group)] | 70% | +1 |
| gb:EAY95519.1 hypothetical protein OsI016752 [Oryza sativa (indica cultivar-group)] | 69% | +1 |
| gb:AAW68439.1 zinc transporter ZIP [Triticum aestivum] | 56% | +1 |
| dbj:BAD18967.1 zinc transporter [Oryza sativa (japonica cultivar-group)] | 49% | +1 |
| dbj:BAD18965.1 zinc transporter [Oryza sativa (japonica cultivar-group)] | 55% | +1 |
| gb:AAX28838.1 zinc transporter protein ZIP2 [Fragaria x ananassa] | 42% | +1 |
| gb:AAP92123.1 iron transporter Fe2 [Oryza sativa (japonica cultivar-group)] | 43% | +1 |
| dbj:BAC21508.1 zinc transporter protein ZIP1 [Oryza sativa (japonica cultivar-group)] | 43% | +1 |
| gb:AAC24197.1 putative zinc transporter [Arabidopsis thaliana] | 38% | +1 |
| ref:NP973762.1 ZIP5 (ZINC TRANSPORTER 5 PRECURSOR) cation transporter [Arabidopsis thaliana] | 36% | +1 |
| emb:CAI77925.2 putative Zn transporter [Thlaspi caerulescens] | 45% | +1 |

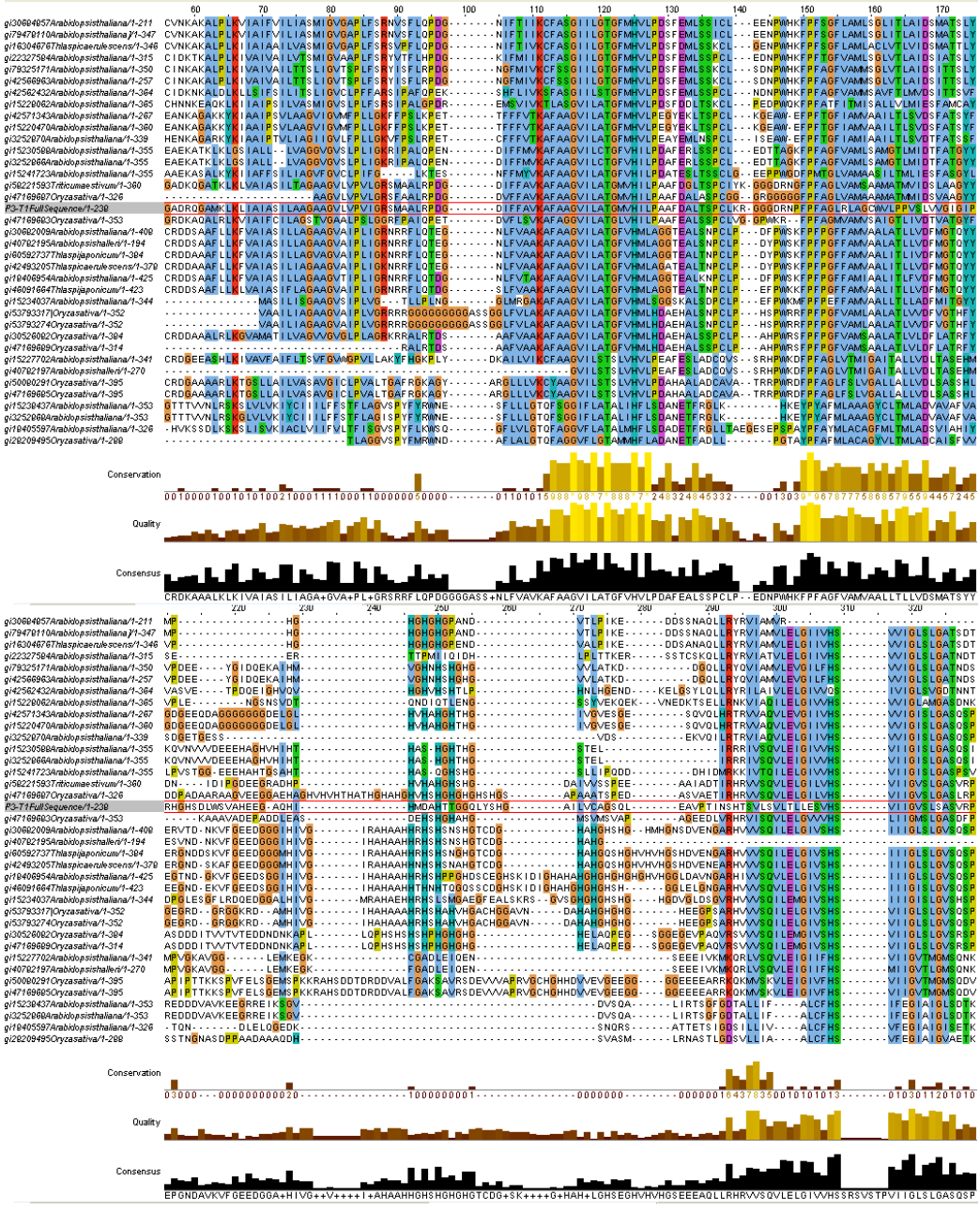

Figure 3.10: The multiple alignment of the protein product of the full mRNA sequence and the known ZIP family proteins of various plants using ClustalX algorithm

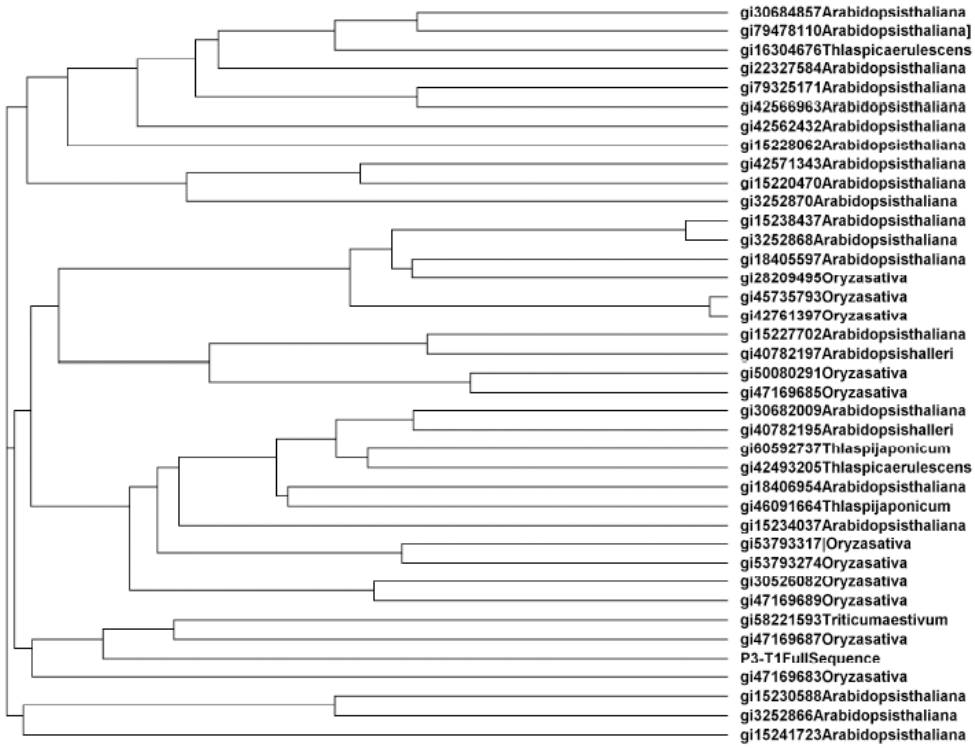


Figure 3.11: The cladogram tree of the ClustalX multiple alignments of the protein product of the full mRNA sequence and the known ZIP family proteins of plants

Table 3.7: ORF of full length mRNA sequence

| Frame | Sequence | Length(aa) |
|---|---|---|
| +1 | Met G A K K H T L Q V L P W L L L F A Q H T A A S A C D C A N T T D G A D R Q G A Met K L K L I A I A S I L A A G A A G V L V P V I G R S Met A A L R P D G D I F F A V K A F A A G L R L A G C W V L P P V S L V V G I G I P S P L K D R R L P G A R H G H S D L W S V A H E E G A Q H I H Met D A H T T G G Q L Y S H G A I L V C A G S Q L E A V P T I N S H T S V L S V L T L L E S V H S V I I G V S L S A S V R P S Stop | 238 |

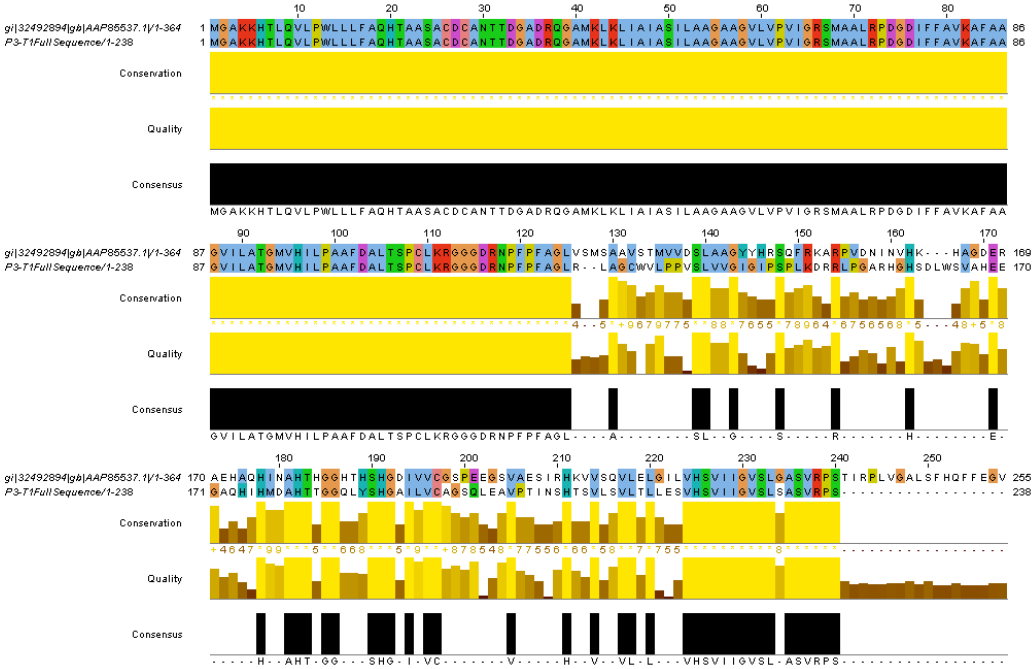


Figure 3.12: The pairwise alignment results of the protein product of the full mRNA sequence and *Oryza sativa* zinc transporter ZIP3(gb:AAP85537.1) using ClustalW algorithm

expressed in the plants without zinc supply and not expressed in the plants grown in 5ppm zinc concentration.

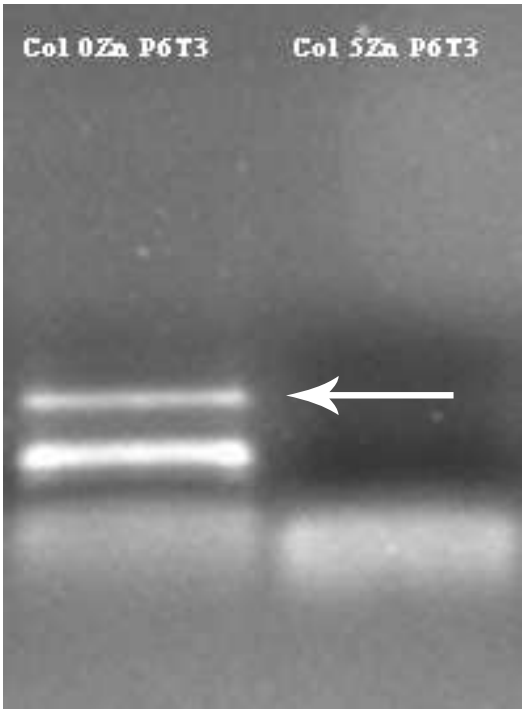


Figure 3.13: Gel electrophoresis results of the band obtained from mRNA differential display of Colonial bentgrass. 50$\mu$lPCR product of P3-T6 primers of the plants grown without zinc on the left and with 5ppm zinc on the right.

The gel electrophoresis results of the fragments isolated from Creeping bentgrass was depicted in Figure 3.14. The fragments indicated with an arrow were extracted from the gel and sequenced (Table 3.9).

The gel electrophoresis results of the two fragments isolated from Velvet bentgrass were shown in Figure 3.14. The fragments indicated with an arrow that were amplified with P2T5 and P3T8 primers were extracted and sequenced (Table 3.10).

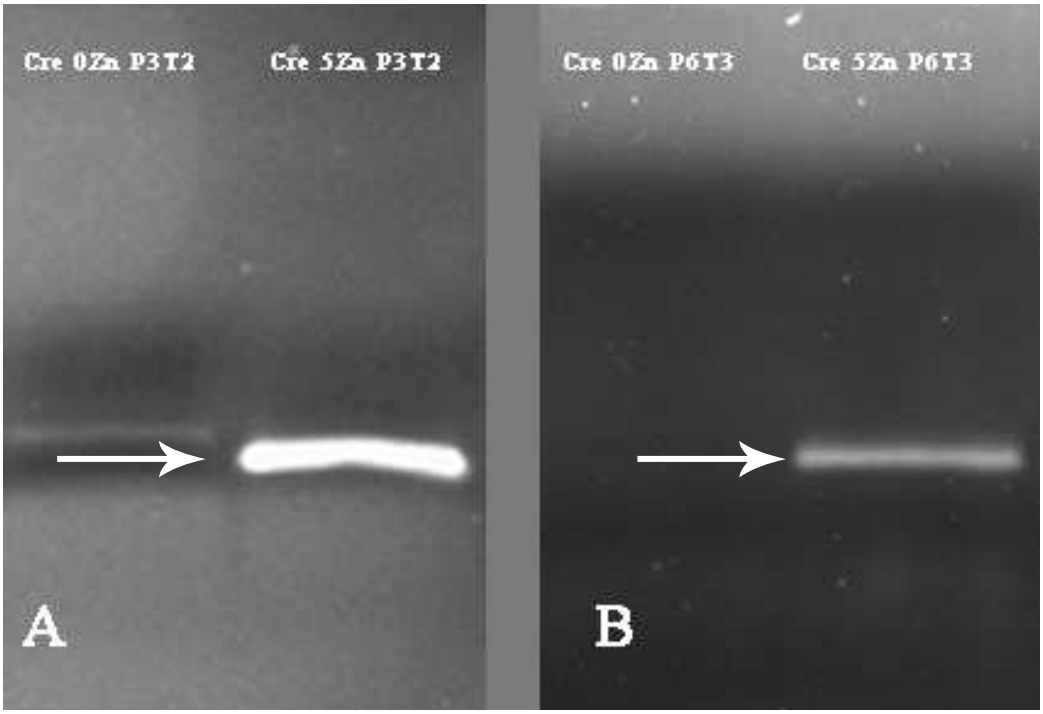


Figure 3.14: Gel electrophoresis results of the bands obtained from mRNA differential display of Creeping bentgrass. (A)50$\mu$l PCR product of P3-T2 primers , (B)50$\mu$lPCR product of P6-T3 primers of the plants grown without zinc on the left and with 5ppm zinc on the right.

Table 3.8: Sequences of the isolated fragments of Colonial bentgrass from greenhouse trial

| Primers | Size(bp) | Sequence |
|---|---|---|
| P6-T3 | 128 | TAT TAA CCC TCA CTA AAT GCT GGG TGA TGC ACT GGC GCT CTA ATA TGC CTA TGC AAT CAG CTT CAT ATT TCT CTT TCT TAA CTT CTA CAT TCG GAC ACT AAA AAA AAA GAT ATC ACT CAG CAT AAT GA |

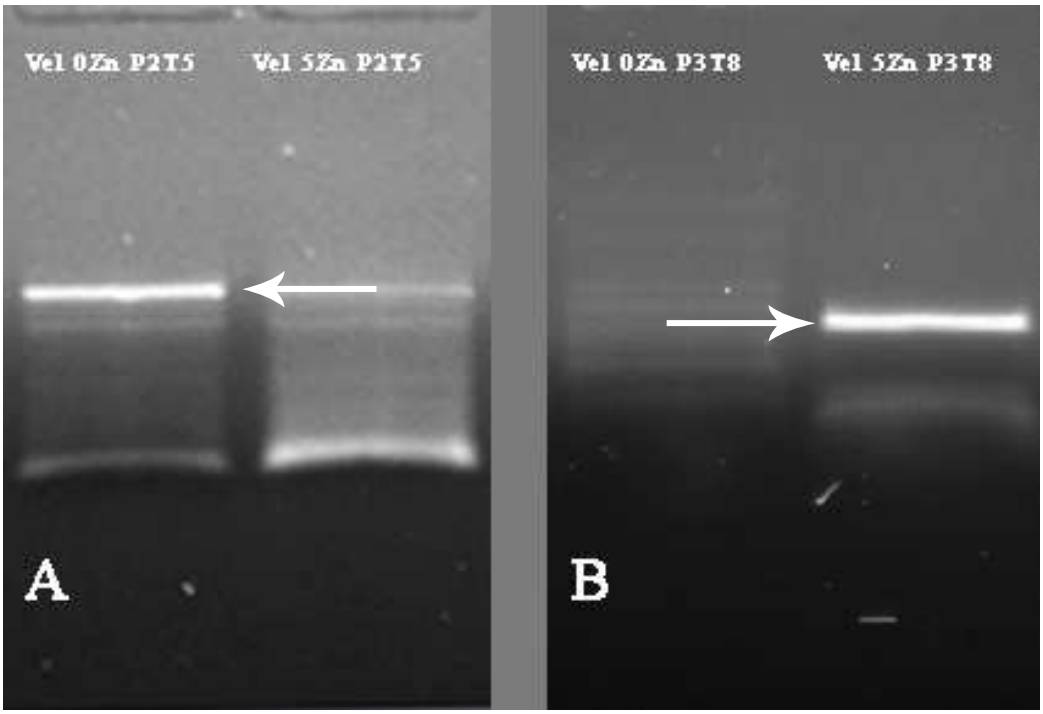


Figure 3.15: Gel electrophoresis results of the bands obtained from mRNA differential display of Velvet bentgrass.(A) 50$\mu$l PCR product of P2-T5 primers, (B)50$\mu$l PCR product of P3-T8 primers of the plants grown without zinc on the left and with 5ppm zinc on the right.

### 3.3.1 BLASTX results

The sequenced fragments isolated from Colonial, Creeping and Velvet bentgrass species were analyzed for their similarity with the sequences in the known protein sequence database using BLASTX algorithm and the results were presented below.

#### BLASTX results of Colonial bentgrass

The fragment amplified with P6-T3 primers in Colonial bentgrass was found to have 85% identity to a protein described as elongation of very long chain fatty acids (FEN1/Elo2, SUR4/Elo3,yeast)-like 4 isolated from Homo sapiens

Table 3.9: Sequences of the isolated fragments of Creeping bentgrass from greenhouse trial

| Primers | Size(bp) | Sequence |
|---|---|---|
| P3-T2 | 145 | TCA TTA CTG CTG AGT GAT ATC TTT TTT TTT ACA CAT ACT GAT CAC AGG TCC CAC CTA TGA AGT TGA TCC GGG GCA CAA CGC TCA GTG TGA TCA GAC GGG ATT CGA CTA TCA TGG ACT TCC CAC CAG CAT TTA GTG AGG GTT AAT A |
| P6-T3 | 221 | TAT TCG ATA TCA CTA GTG AAT TCG CGG CCC GCC TGC AGG TCG ACC ATA CTG GGA GAG CTC CCA ACG CGT TGG ATG CAT AGC TTG AGT ATT CTA TAG TGT CAC CTA AAT AGC TTG AGC GTA ATC ATG GTC ATA GCT GTT CCT GTG TGA AAT TGT ATC CGC TCA CAA TTC CAC ACA ACA TAC GAG CCG GAA GCA TAA AGT GTA AAG CCT GGG GTG CCT AAT GA |

but highly conserved in various organisms (Table 3.11). It also showed 100% identity to a region of putative myosin heavy chain identified in Dendrobium grex Madame Thong-In. Another protein that the fragment showed 87% similarity was CRK6 (CYSTEINE-RICH RLK 6) of Arabidopsis thaliana that is known as member of phosphotransferases of the serine or threonine-specific kinase subfamily.

**BLASTX results of Creeping bentgrass**

For the two fragments isolated from Creeping bentgrass, BLASTX results were shown in Table 3.12. The fragment amplified with P3-T2 primers showed 83% identity to the hypothetical protein OsJ029202 and an unknown protein of Oryza sativa which both have R3H domain of encore-like proteins. It interestingly showed 90% similarity to the Zn-dependent

Table 3.10: Sequences of the isolated fragments of Velvet bentgrass from greenhouse trial

| Primers | Size(bp) | Sequence |
|---|---|---|
| P2-T5 | 327 | TAT TAA CCC TCA CTA AAT CGG TTC ATA GTT GAG AGG GGA ATA GTA TAA CAT AGG AAG ACC CTT TAT CGA TAC TAA GAA CAA AAT GGT TTT TTT TGA TTG GAT TAG GAA TTC CCT CTT TTC TTT TTT TAA TCC TTT TCT CCT TTT TCT TTT CTA TAC CTC TAA CCC ACG AAT CTT TCT TAA TCT TAT CCA ATT TCC CTT ACT TTT TCT TAT AGT TAT ACA TAC AAT TAT GTA TGT ATT ATA TGA CCA ACT TTC TAT GGG TCA CAT AGA CAT CCA AAT AAG CAG TAG AAC TGA CAC GGG GAA AAA AAA AGA TAT CAC TCA GCA TAA TGA |
| P3-T8 | 146 | TAT TAA CCC TCA CTA AAT GCT GGG TGG TTT TGG GCT ACA ATA GAT GAC GAG GGA ACT AGT TAT TAA GTG TGC TTG AAA CCT ATC CAT GGT ACA TTC ACA GAA TTG AGC GAC GGT GGC AAA AAA AAA GAT ATC ACT CAG CAT AAT GA |

Table 3.11: BlastX results of Colonial bentgrass greenhouse trial using NCBI BLASTX algorithm with Blossom80 and PAM30 matrices

| Primers | BLASTX hit | Identity | Frame |
|---|---|---|---|
| P6-T3 | gb:AAH38506.1 Elongation of very long chain fatty acids (FEN1/Elo2, SUR4/Elo3,yeast)-like 4 [Homo sapiens] | 85% | +2 |
| | gb:AAD20814.1 putative myosin heavy chain [Dendrobium grex Madame Thong-In] | 100% | +3 |
| | ref:NP849426.1 CRK6 (CYSTEINE-RICH RLK 6) [Arabidopsis thaliana] | 87% | +3 |

proteases region (SpoIVFB) of a peptidase isolated from *Crocosphaera watsonii*(cyanobacteria). It has 84% similarity to putative iron compound ABC transporter, permease protein from Clostridium difficile and the same region also showed similarity to a hypothetical protein from the same bacteria which also has a ABC-type enterochelin transport system, permease component. The same region was found in a ferric anguibactin transport system permease protein FatC of *Vibrio fischeri* (Table 3.12).

The fragment amplified with P6-T3 primers had 90% identity to a manganese superoxide dismutase isolated from Taiwanofungus camphoratus. It also showed 78% similarity to a putative transcriptional regulator, Crp/Fnr family of Burkholderia cepacia (Table 3.12).

**BLASTX results of Velvet bentgrass**

For the two fragments isolated from Velvet bentgrass, BLASTX results were shown in Table 3.13. The fragment amplified with P2-T5 primers found to have 60% idendity to cytochrome c oxidase subunit III of Aleurodicus dugesii and 100% identity to the same putative casein kinase I of Dendrobium grex Madame Thong-In as the fragments from creeping and colonial bentgrass.

The fragment amplified with P3-T8 primers showed 61% identity to putative copper/zinc superoxide dismutase copper chaperone of Dendrobium grex Madame Thong-In and also very interstingly it showed 71% identity to glutathione-independent formaldehyde dehydrogenase of Methanosarcina mazei which has a zinc-binding dehydrogenase domain(Table 3.13).

### 3.3.2 ORF regions of the obtained sequences

The open reading frames of the obtained sequences from Colonial, Creping and Velvet bentgrass were detected using ORF Finder algorithm of NCBI.

Table 3.12: BlastX results of Creeping bentgrass greenhouse trial using NCBI BLASTX algorithm with Blossom80 and PAM30 matrices

| Primers | BLASTX hit | Identity | Frame |
|---|---|---|---|
| P3-T2 | gb:EAZ45719.1 hypothetical protein OsJ029202 [Oryza sativa (japonica cultivar-group)] | 83% | +2 |
| | dbj:BAD46211.1 unknown protein [Oryza sativa (japonica cultivar-group)] | 83% | +2 |
| | ref:ZP00518540.1 CBS:Peptidase M50 [Crocosphaera watsonii WH 8501] | 90% | +1 |
| | ref:YP001088149.1 putative iron compound ABC transporter, permease protein [Clostridium difficile 630] | 84% | -1 |
| | ref:ZP01803509.1 hypothetical protein CdifQ04001892 [Clostridium difficile QCD-32g58] | 84% | -1 |
| | ref:YP206783.1 ferric anguibactin transport system permease protein FatC [Vibrio fischeri ES114] | 84% | -1 |
| P6-T3 | emb:CAD42938.2 manganese superoxide dismutase [Taiwanofungus camphoratus] | 90% | -3 |
| | ref:YP775527.1 putative transcriptional regulator, Crp/Fnr family [Burkholderia cepacia AMMD] | 78% | -2 |

Table 3.13: BlastX results of Velvet bentgrass greenhouse trial using NCBI BLASTX algorithm with Blossom80 and PAM30 matrices

| Primers | BLASTX hit | Identity | Frame |
|---|---|---|---|
| P2-T5 | ref:YP026057.1 cytochrome c oxidase subunit III [Aleurodicus dugesii] | 60% | +3 |
| | gb:AAD20819.1 putative casein kinase I [Dendrobium grex Madame Thong-In] | 100% | -3 |
| P3-T8 | gb:AAC79870.1 putative copper/zinc superoxide dismutase copper chaperone [Dendrobium grex Madame Thong-In] | 61% | +1 |
| | ref:NP632773.1 Glutathione-independent formaldehyde dehydrogenase [Methanosarcina mazei Go1] | 71% | -3 |

**ORF regions of the obtained sequences from Colonial bentgrass**

ORF finder analysis shoed that the fragment amplified with the same primers had an eight amino acids long ORF in the frame 2, a twenty four amino acids long ORF in the frame 3 and a twelve and five amino acids long ORF in the frame -3 (Table 3.14). The fragment amplified with P2-T4 primers had one ORF that had a length of 19 amino acids in the frame 3 (Table 3.14).

All the open reading frames found for Colonial bentgrass were too short except the twenty four amino acids long ORF for the fragment amplified with P6-T3 primers. This protein sequence had two histidines that was known to be reach in metal binding proteins.

**ORF regions of the obtained sequences from Creeping bentgrass**

The ORFs found for the fragments isolated from Creeping bentgrass were shown in Table 3.15. The fragment amplified with P3-T2 primers had a twenty eight amino acids long ORF in the frame two, a twenty seven amino

Table 3.14: ORFs of the sequences of Colonial bentgrass

| Primers | Frame | Sequence | Length(aa) |
|---|---|---|---|
| P6-T3 | 2 | Met L G D A L A L Stop | 8 |
| | 3 | Met H W R S N Met P Met Q S A S Y F S F L T S T F G H Stop | 24 |
| | -3 | Met L S D I F F F S V R Met Stop | 12 |
| | -3 | Met K L I A Stop | 5 |

acids long ORF in the frame -1 and a ten amino acids long ORF in the frame -2. The fragment that was amplified with P6-T3 primers had four ORFs in the frames 1,-1,-2 and -3 that were 7, 10,21 and 21 amino acids in length, respectively.

The longest amino acid sequence found for Creeping bentgrass had 28 amino acids (Table 3.15). The sequence was searched for conserved motifs using Motif Scan algorithm and was found to have a cAMP- and cGMP-dependent protein kinase phosphorylation site in the region 13-16 (R R D S), Casein kinase II phosphorylation site in the region 17-20 (T I M D). The 21 amino acids long ORF of the fragment (P6-T3) interestingly showed a Zinc finger DPH-type profile for the whole sequence (Figure 3.16).

**ORF regions of the obtained sequences from Velvet bentgrass**

The ORFs found for the fragments isolated from Velvet bentgrass were listed in Table 3.16. The fragment amplified with P2-T5 primers had five ORFs in the frames 3,-1,-2,-3 and -3 of 11,12,7,28 and 7 amino acids in length, respectively. The fragment amplified with P3-T8 primers had three short ORFs in the frame 2 and a fourty two amino acids long ORF in the frame -3. The 28 amino acids lond ORF of P2-T5 fragment showed a similarity to

Table 3.15: ORFs of the sequences of Creeping bentgrass

| Primers | Frame | Sequence | Length(aa) |
|---|---|---|---|
| P3-T2 | 3 | Met K L I R G T T L S V I R R D S T I Met D F P P A F S E G Stop | 28 |
| | -1 | Met I V E S R L I T L S V V P R I N F I G G T C D Q Y V Stop | 27 |
| | -2 | Met C K K K D I T Q Q Stop | 10 |
| P6-T3 | 1 | Met H S L S I L Stop | 7 |
| | -1 | Met T Met I T L K L F R Stop | 10 |
| | -2 | Met L P A R Met L C G I V S G Y N F T Q E Q L Stop | 21 |
| | -3 | Met H P T R W E L S Q Y G R P A G G P R I H Stop | 21 |

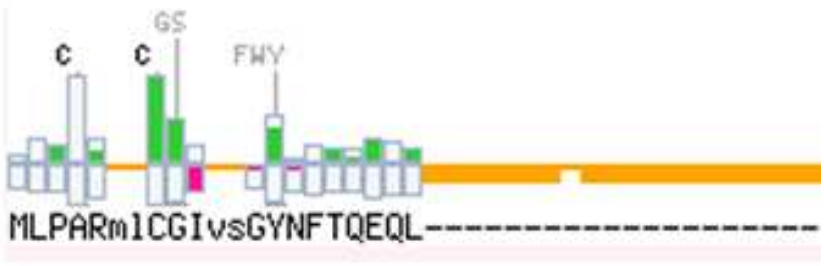


Figure 3.16: The motif predicted for the twenty one amino acids long ORF sequence of the fragment amplified with P6-T3 primers in the Creeping bentgrass found by Motif Scan algorithm

the NERD domain profile (Figure 3.17). The longest ORF found for Velvet bentrgrass (42 amino acids) had three cysteines and one histidine however did not have a significant hit in the Motif Scan.

Table 3.16: ORFs of the sequences of Velvet bentgrass

| Primers | Frame | Sequence | Length(aa) |
|---|---|---|---|
| P2-T5 | 3 | Met Y Y Met T N F L W V T Stop | 11 |
| | -1 | Met L Y Y S P L N Y E P I Stop | 12 |
| | -2 | Met N R F S E G Stop | 7 |
| | -3 | Met L S D I F F F P R V S S T A Y L D V Y V T H R K L V I Stop | 28 |
| | -3 | Met Y N Y K K K Stop | 7 |
| P3-T8 | 2 | Met L G G F G L Q Stop | 8 |
| | 2 | Met T R E L V I K C A Stop | 10 |
| | 2 | Met V H S Q N Stop | 6 |
| | -3 | Met L S D I F F F A T V A Q F C E C T Met D R F Q A H L I T S S L V I Y C S P K P P S I Stop | 42 |

### 3.3.3 Pairwise alignment of the fragments that were amplified with the same primer sets

There were two primer sets that amplified a fragment both for Colonial and Creeping bentgrass and these fragments were aligned using ClustalW algorithm of EBI. The pairwise alignment of the fragments were shown in Figure 3.18. The results indicated that the fragments are similar in sequence.

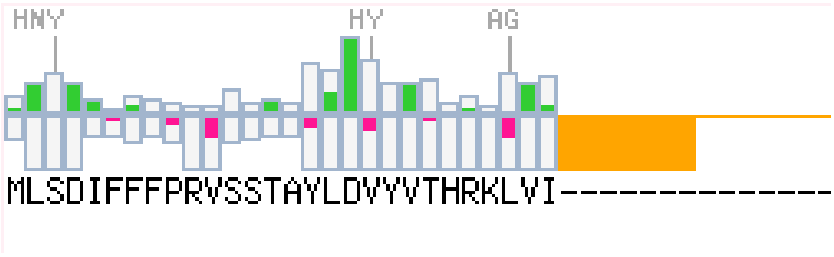


Figure 3.17: The motif predicted for the twenty eight amino acids long ORF sequence of the fragment amplified with P2-T5 primers in the Velvet bentgrass found by Motif Scan algorithm

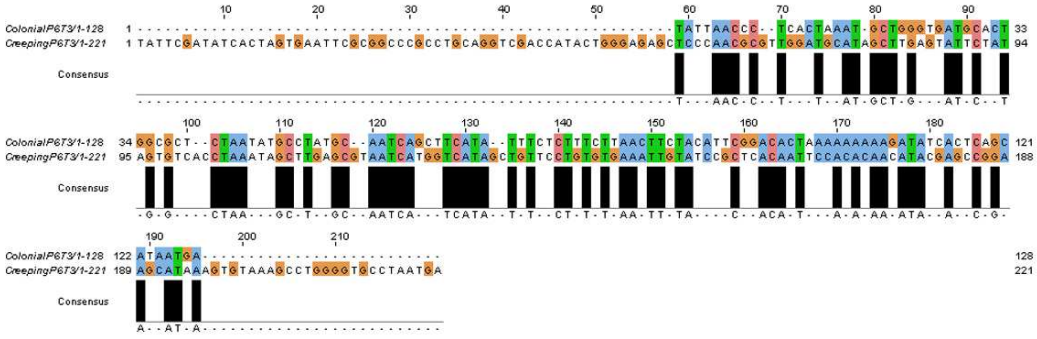


Figure 3.18: Pairwise alignment of the fragments amplified with P6-T3 primers both in Colonial and Creeping bentgrass

# Chapter 4

# Discussion

## 4.1 Physiological analysis

The concentration and content of zinc in the seeds of Creeping, Colonial and Velvet bentgrass was presented in Section 3.1.1. Since zinc concentration of the seeds has huge effect on growth of seedlings after germination, it was important to know the zinc concentration of seeds for all genotypes tested [56]. Velvet bentgrass seeds had the highest amount of zinc among the three species where as the other two had almost the same zinc concentration, indicating that high susceptibility of Velvet to zinc deficiency was not related to the low seed zinc concentration.

According to the dry weights of plants after four weeks of growth under zinc deficiency presented in Section 3.1.2, Velvet bentgrass was almost unresponsive to 0.1ppm zinc application probably due to its high amount of zinc in the seeds or poor genetic capacity of zinc acquisition from soil. Creeping bentgrass was found to be the most tolerant species to zinc deficiency when compared to the others used in this study. . In addition to the earliest research on *Agrostis tenuis* , this data suggested that Creeping bentgrass is also tolerant to zinc deficiency among Agrostis species. The experiment also showed that the most susceptible species among the three was Velvet

bentgrass.

Zn concentration of Colonial bentgrass grown without zinc was much higher than it was expected (Figure 3.3). This is probably due to soil contamination before the ICP measurements rather than zinc contamination in the soil because the same deviance was not observed for the dry weights of the plants. Soil contamination to the samples was also supported by the high level of Al amount.

## 4.2 Identification of Zn responsive genes by using mRNADD in Creeping, Colonial and Velvet bentgrass

By using mRNADD method, nine zinc responsive transcripts, six in Creeping, one in Colonial and two in Velvet bentgrass, that were differentially expressed in response to zinc deficiency, have been identified. The experiments were repeated for several times and only the absolutely reproducible fragments have been considered to be specific and analyzed further. The non-reproducible fragments were omitted. Majority of the identified transcripts have partial similarities with the previously identified metal binding proteins. These results clearly indicated that mRNADD tool worked perfectly to identify Zn responsive genes those can readily be located on molecular linkage maps to identify the chromosomal location of Zn responsive genes on grass genome.

The differentially expressed genes that were identified were thought to be partial mRNA sequences although most of them have ORF regions. To obtain the full sequences, RACE method should be used by designing gene specific primers for each of the fragments. Obtaining the full sequences of the transcripts will provide more information about the homology and orthology

with the previously identified proteins. ORF regions of the full mRNAs can be used to translate the product in a model organism for structural and biochemical characterizations.

## 4.3 Identification and characterization of ZIP family transporter in Creeping bentgrass

The fragment isolated from Creeping bentgrass that was amplified by P3-T1 primers was found to be one of the most interesting fragment due its bigger size in comparison and its similarity with three ZIP transporters with around 50% identity. Hence, the differentially expressed gene was further analysed. The real-time PCR results for the expression analysis of the fragment clearly indicated that its expression level was highly affected by the Zn concentration in the growth medium. The real-time PCR was performed for total cDNAs isolated from both tissue culture trial and green house trial and the data indicated that the difference in the expression levels are almost the same for both. It has been known that the expression of genes encoding the plant ZIP transporters appears to be affected by zinc or iron deficiency which was also observed in this experiment ( [34, 35]). The full length mRNA sequence was found to be homologous to ZIP zinc transporter family proteins which are mostly membrane proteins involved in transportation of the zinc. Decrease in the expression level of this gene can be explained by its role, so if there is more zinc to transport in the plant the expression level of the gene increases.

The fragment that was obtained by P3-T1 primers had two specific ORFs and these were cloned to an expression vector and expressed in *E. coli*. However, both protein products were not obtained probably because they could not complete their proper folding and become targets of protease activity. As a result of this assumption, the full mRNA sequence of the fragment was

obtained by RACE.

The full length mRNA sequence (AsZIP) obtained by RACE was found to be a good candidate to be Creeping bentgrass homologous of ZIP family metal transporters detected in many organisms including plants, human and bacteria. This result was supported with BLASTX results and the CLUSTALX alignments with the known proteins of the ZIP family (Table 3.6, Figure 3.10).

BLASTX results indicated that the protein product was highly similar to zinc transporter ZIP3 identified in *Oryza sativa*(OsZIP3,gbAAP85537.1)( [57, 58]). According to Ramesh *et al.*, the cDNAs was partially complemented to a yeast mutant, deficient in zinc uptake at low Zn concentrations. They claimed that OsZIP3 was expressed under control conditions, but gene expression was slightly up-regulated when zinc was removed from the medium and concluded that and that OsZIP3 is constitutively active and involved in overall cell zinc homeostasis, particularly in leaves. Their findings in *Oryza sativa* are totally consistent with this experiment and makes OsZIP3 of *Oryza sativa* the best reference for the novel gene identified for the first time in Agrostis. To compare the functional similarity between the two proteins, functional complementary studies will be performed as for OsZIP3.

The physiological analysis indicated that Creeping bentgrass was the most tolerant species to zinc deficiency when compared to Colonial and Velvet bentgrass. Due to its similarity with OsZIP3, AsZIP is predicted to increase zinc uptake and translocation. Hence, the expression of AsZIP gene in Creeping bentgrass may contribute to its tolerance level to zinc deficiency.

# Chapter 5

# Conclusion

This study demonstrated that Creeping bentgrass was the most tolerant grass species to zinc deficiency when compared to Colonial and Velvet bentgrass used in this study. On the other hand the most susceptible species was Velvet bentgrass although its growth was slightly less than Colonial bentgrass under zinc deficiency.

Nine transcripts in total were detected using mRNA differential display technique whose expression levels either increased or decreased under zinc deficiency. The identified transcripts are found to be a portion of corresponding mRNAs of zinc responsive genes. The full length mRNA sequence in Creeping bentgrass , whose expression level decreased by $2^5$ and $2^6$ fold, in tissue culture and green house trials, respectively, was obtained by 3' and 5' RACE.

The full length mRNA sequence is found to be homologous to ZIP zinc transporter family proteins which are mostly membrane proteins involved in transportation of the zinc after the uptake. This is the first study that a ZIP family zinc transporter is identified in Agrostis species. Functional analysis of the protein product of the novel gene will be performed.

# Bibliography


[1] EA. Kellogg. Evolutionary History of the Grasses. *Plant Physiol*, 125:1198–1205, 2001.

[2] HL. Shantz. The Place of Grasslands in the Earth's Cover. *Ecology*, 35(2):143–145, 1954.

[3] AS. Hitchcock. *Manual of the Grasses of the United States, Vol. 1*. Dover Publications, 1971.

[4] H. Budak, S. Su, and N. Ergen. Revealing constitutively expressed resistance genes in Agrostis species using PCR-based motif-directed RNA fingerprinting. *Genetical Research*, 88(03):165–175, 2007.

[5] FC. Belanger, TR. Meagher, PR. Day, K. Plumley, and WA. Meyer. Interspecific Hybridization between Agrostis stolonifera and Related Agrostis Species under Field Conditions. *Crop Science*, 43(1):240–246, 2003.

[6] AD Bradshaw. Populations of Agrostis tenuis resistant to lead and zinc poisoning. *Nature*, 169(4313):1098, 1952.

[7] EA. Gladkov. Effect of complex interaction between heavy metals on plants in a megalopolis. *Russian Journal of Ecology*, 38(1):68–71, 2007.

[8] RD. Graham, RM. Welch, and HE. Bouis. Addressing micronutrient malnutrition through enhancing the nutritional quality of staple foods: Principles, perspectives and knowledge gaps. *Advances in Agronomy*, 70:77–142, 2001.

[9] RJP. Williams. An introduction to the biochemistry of zinc. *Zinc in Human Biology*, 4:15–31, 1989.

[10] KA. McCall, C. Huang, and CA. Fierke. Function and Mechanism of Zinc Metalloenzymes. *Journal of Nutrition*, 130:1437–1446, 2000.

[11] A. Klug and D. Rhodes. Zinc fingers: a novel protein motif for nucleic acid recognition. *Trends Biochem. Sci*, 12(464-469):9, 1987.

[12] JM. Berg and Y. Shi. The Galvanization of Biology: A Growing Appreciation for the Roles of Zinc. *Science*, 271(5252):1081, 1996.

[13] M. Hambidge. Human Zinc Deficiency. *Journal of Nutrition*, 130:1344–1349, 2000.

[14] JK. Chesters. Metabolism and biochemistry of zinc. *Clinical, Biochemical, and Nutritional Aspects of Trace Elements*, 6:221–238, 1982.

[15] CJ. Frederickson, SW. Suh, D. Silva, and RB. Thompson. Importance of zinc in the central nervous system: the zinc-containing neuron. *J Nutr*, 130(5S Suppl):1471S–83S, 2000.

[16] RE. Burch, HK. Hahn, and JF. Sullivan. Newer aspects of the roles of zinc, manganese, and copper in human nutrition. *Clin Chem*, 21(4):501–20, 1975.

[17] AS. Prasad, JA. Halsted, and M. Nadimi. Syndrome of iron deficiency anemia, hepatosplenomegaly, hypogonadism, dwarfism and geophagia. *The Journal of Trace Elements in Experimental Medicine*, 14(2):121–144, 2001.

[18] KH. Brown. Effect of infections on plasma zinc concentration and implications for zinc status assessment in low-income countries. *Clin Nutr*, 68:425–9, 1998.

[19] BJ. Alloway. Zinc in Soils and Crop Nutrition. *International Zinc Association: Brussels, Belgium*, 2004.

[20] AF. López-Millán, DR. Ellis, and MA. Grusak. Identification and Characterization of Several New Members of the ZIP Family of Metal Ion Transporters in Medicago Truncatula. *Plant Molecular Biology*, 54(4):583–596, 2004.

[21] BJ. van der Zaal, LW. Neuteboom, JE. Pinas, AN. Chardonnens, H. Schat, JAC. Verkleij, and PJJ. Hooykaas. Overexpression of a Novel Arabidopsis Gene Related to Putative Zinc-Transporter Genes from Animals Can Lead to Enhanced Zinc Resistance and Accumulation. *Plant Physiology*, 119(3):1047–1056, 1999.

[22] H. Marschner. *Mineral nutrition of higher plants*. Academic Press San Diego, 1995.

[23] PH. Brown, I. Cakmak, and Q. Zhang. Form and function of zinc in plants. *Zinc in Soils and Plants. Ed. AD Robson*, pages 107–118, 1993.

[24] RD. Graham, JS. Ascher, and SC. Hynes. Selecting zinc-efficient cereal genotypes for soils of low zinc status. *Plant and Soil*, 146(1):241–250, 1992.

[25] RM. Welch, MJ. Webb, and JF. Loneragan. Zinc in membrane function and its role in phosphorus toxicity. *Plant Nutrition*, pages 710–715, 1982.

[26] I. Cakmak and H. Marschner. Enhanced Superoxide Radical Production in Roots of Zinc-Deficient Plants. *Journal of Experimental Botany*, 39(10):1449, 1988.

[27] P. Barak and PA. Helmke. The chemistry of zinc. *Proceedings of the International Symposium on Zinc in Soils and Plants.Developments in Plant and Soil Sciences*, 55:1–13, 1993.

[28] AF. Lopez-Millan, DR. Ellis, and MA. Grusak. Effect of zinc and manganese supply on the activities of superoxide dismutase and carbonic anhydrase in Medicago truncatula wild type and raz mutant plants. *Plant Science*, 168(4):1015–1022, 2005.

[29] EKS. Nambiar. The Uptake of Zinc-65 by Oats in Relation to Soil Water Content and Root Growth. *Australian Journal of Soil Research*, 14(1):67–74, 1976.

[30] HU. Neue, C. Quijano, D. Senadhira, and T. Setter. Strategies For Dealing With Micronutrent Disorders And Salinity In Lowland Rice Systems. *Field crops research*, 56(1-2):139–155, 1998.

[31] FM. Chaudhry and JF. Loneragan. Zinc absorption by wheat seedlings: 1. Inhibition by macronutrient ions in short-term experiments and its relevance to long-term zinc nutrition. *Soil Sci. Soc. Amer. Proc. 36*, 323:327, 1972.

[32] P. Maser, S. Thomine, JI. Schroeder, JM. Ward, K. Hirschi, H. Sze, IN. Talke, A. Amtmann, FJM. Maathuis, and D. Sanders. Phylogenetic Relationships within Cation Transporter Families of Arabidopsis. *Plant Physiology*, 126(4):1646–1667, 2001.

[33] YO. Korshunova, D. Eide, W. Gregg Clark, M. Lou Guerinot, and HB. Pakrasi. The IRT1 protein from Arabidopsis thaliana is a metal transporter with a broad substrate range. *Plant Molecular Biology*, 40(1):37–44, 1999.

[34] D. Eide, M. Broderius, J. Fett, and ML. Guerinot. A Novel Iron-Regulated Metal Transporter From Plants Identified By Functional Expression In Yeast. *Proceedings of the National Academy of Sciences of the United States of America*, 93(11):5624–5628, 1996.

[35] N. Grotz, T. Fox, E. Connolly, W. Park, ML. Guerinot, and D. Eide. Identification of a Family of Zinc Transporter Genes from Arabidopsis that Respond to Zinc Deficiency. *Proceedings of the National Academy of Sciences of the United States of America*, 95(12):7220–7224, 1998.

[36] NS. Pence, PB. Larsen, SD. Ebbs, DLD. Letham, MM. Lasat, DF. Garvin, D. Eide, and LV. Kochian. The molecular physiology of heavy metal transport in the Zn&cjs1134; Cd hyperaccumulator Thlaspi caerulescens. *Proceedings of the National Academy of Sciences of the United States of America*, pages 4956–60, 2000.

[37] U. Eckhardt, A. Mas Marques, and TJ. Buckhout. Two iron-regulated cation transporters from tomato complement metal uptake-deficient yeast mutants. *Plant Molecular Biology*, 45(4):437–448, 2001.

[38] GGS. Holmgren, MW. Meyer, RL. Chaney, and RB. Daniels. Cadmium, lead, zinc, copper, and nickel in agricultural soils of the United States of America. *Journal of environmental quality*, 22(2):335–348, 1993.

[39] H. Zhao and D. Eide. The Yeast ZRT1 Gene Encodes the Zinc Transporter Protein of a High-Affinity Uptake System Induced by Zinc Limitation. *Proceedings of the National Academy of Sciences of the United States of America*, 93(6):2454–2458, 1996.

[40] MA. Grusak. Enhancing Mineral Content in Plant Food Products. *Journal of the American College of Nutrition*, 21(90003):178–183, 2002.

[41] MA. Grusak, JN. Pearson, and E. Marentes. The physiology of micronutrient homeostasis in field crops. *Field Crops Research*, 60(1):41–56, 1999.

[42] WL. Lindsay. Zinc in soils and plant nutrition. *Adv. Agron*, 24:147–186, 1972.

[43] ML. Guerinot. The ZIP family of metal transporters. *Biochim Biophys Acta*, 1465(1-2):190–8, 2000.

[44] BH. Eng, ML. Guerinot, D. Eide, and MH. Saier. Sequence Analyses and Phylogenetic Characterization of the ZIP Family of Metal Ion Transport Proteins. *Journal of Membrane Biology*, 166(1):1–7, 1998.

[45] LA. Gaither and DJ. Eide. Functional Expression of the Human hZIP2 Zinc Transporter. *Journal of Biological Chemistry*, 275(8):5560–5564, 2000.

[46] L. Huang, CP. Kirschke, and J. Gitschier. Functional Characterization of a Novel Mammalian Zinc Transporter, ZnT6. *Journal of Biological Chemistry*, 277(29):26389–26395, 2002.

[47] EL. Connolly, JP. Fett, and ML. Guerinot. Expression of the IRT1 Metal Transporter Is Controlled by Metals at the Levels of Transcript and Protein Accumulation. *The Plant Cell Online*, 14(6):1347–1357, 2002.

[48] LA. Gaither and DJ. Eide. Eukaryotic zinc transporters and their regulation. *BioMetals*, 14(3):251–270, 2001.

[49] P. Liang and AB. Pardee. Differential display of eukaryotic messenger RNA by means of the polymerase chain reaction. *Science*, 257(5072):967–971, 1992.

[50] P. Liang, D. Bauer, L. Averboukh, P. Warthoe, M. Rohrwild, H. Muller, M. Strauss, and AB. Pardee. Analysis of altered gene expression by differential display. *Methods Enzymol*, 254:304–21, 1995.

[51] N. Ergen, G. Dinler, RC. Shearman, and H. Budak. Identifying,cloning and structural analysis of differentially expressed genes upon *Puccinia* infection of *Festuca rubra* var. *rubra* . *Gene*, 393:145–152, 2007.

[52] SW. Shin, SS. Park, DS. Park, MG. Kim, SC. Kim, PT. Brey, and HY. Park. Isolation and characterization of immune-related genes from the fall webworm, Hyphantria cunea, using PCR-based differential display and subtractive cloning. *Insect Biochem Mol Biol*, 28(11):827–37, 1998.

[53] Cebeci O. Molecular characterization and expression profiling of cd-responsive genes in triticum durum. Master's thesis, Sabanci University, 2006.

[54] P. Liang. A decade of differential display. *Biotechniques*, 33(2):338–344, 2002.

[55] N. Terry and G. Low. Leaf chlorophyll content and its relation to the intracellular localization of iron. *J Plant Nutr*, 5:301–310, 1982.

[56] A. Yilmaz, H. Ekiz, B. Torun, I. Gultekin, S. Karanlik, SA Bagci, and I. Cakmak. Effect of different zinc application methods on grain yield and zinc concentration in wheat cultivars grown on zinc-deficient calcareous soils. *Journal of plant nutrition*, 20(4-5):461–471, 1997.

[57] SA. Ramesh, R. Shin, DJ. Eide, and DP. Schachtman. Differential Metal Selectivity and Gene Expression of Two Zinc Transporters from Rice. *Plant Physiology*, 133(1):126–134, 2003.

[58] H. Zhao and D. Eide. The ZRT2 Gene Encodes the Low Affinity Zinc Transporter in Saccharomyces cerevisiae. *Journal of Biological Chemistry*, 271(38):23203–10, 1996.

# Appendix A

# Appendix

## A.1 Chemicals and Kits

| Chemical | Company | Catalog No. |
|---|---|---|
| 2-Mercaptaethanol | Aldrich, Germany | M370-1 |
| 2-Propanol | MerckKGaA, Germany | 1.00995 |
| 6X Loading dye | Fermentas, Canada | RO611 |
| Acetic acid | Riedel-de Haen, Germany | 27225 |
| Acetone | MerckKGaA, Germany | 100013 |
| Acrylamide 30%-0.8% Bi-acrylamide | Sigma, Germany | A3699 |
| Acetic acid | Riedel-de Haen, Germany | 27225 |
| Agarose low EEO | AppliChem GmbH, Germany | A2114 |
| Ampicillin sodium salt | AppliChem GmbH, Germany | A0839 |
| Bromophenol blue | Applichem, Germany | A3640 |
| aTaq DNA polymerase | Promega, USA | M1245 |
| Chloroform | Amresco Inc., USA | 0757 |
| Coomassie brilliant blue | Fluka, Switzerland | 27816 |
| DNaseI | Fermentas, Canada | EN0521 |
| dNTP mix | Promega, USA | U1515 |
| Ethanol | MerckKGaA, Germany | 1.00986 |
| Ethidium bromide | MerckKGaA, Germany | 1.11608 |
| GeneRacer Kit | Invitrogen, USA | L1502-02 |
| GeneRuler 100bp DNA ladder plus | Fermentas, Canada | SM0321 |
| Glycerol 87% | Riedel-de Haen, Germany | 15523 |

| | | |
|---|---|---|
| Hybond PVDF membrane | Amersham, Sweeden | RPN2020F |
| Hydrochloric acid 37% | MerckKGaA, Germany | 100314 |
| IPTG | Fermentas, Canada | RO393 |
| LB broth | Sigma-Aldrich Co., USA | L3022 |
| Magnesium chloride | Riedel-de Haen, Germany | 13152 |
| Magnesium sulfate | Riedel-de Haen, Germany | 13246 |
| Methanol | Riedel-de Haen, Germany | 24229 |
| Oligo(dT) Primer | Invitrogen, USA | L3147 |
| Omniscript RT Kit | Qiagen, USA | 20511 |
| Pageruler protein ladder | Fermentas, Germany | SM0661 |
| PGEM-T Vector System II | Promega, USA | A3610 |
| Qiaprep Spin Miniprep Kit | Qiagen, USA | 27106 |
| Qiaquick Gel Extraction Kit | Qiagen, USA | 28706 |
| RNaseOUT | Invitrogen, USA | 10777-019 |
| Sodium chloride | Riedel-de Haen, Germany | 13423 |
| Tetramethylethylenediamine | Sigma, Germany | T-7029 |
| Tris | Fluka, Switzerland | 93349 |
| Trizol Reagent | Invitrogen, USA | 15596 |
| X-Gal | Promega, USA | V3941 |

## A.2 Equipment

**Autoclave** Hirayama, Hiclave HV-110, Japan.

**Balance** Sartorius, BP610, BP221S, BP221D, Germany.

**Blot Module** Novex, X Cell II Blot Module, USA.

**Centrifuge** Eppendorf, 5415R, Germany; Hitachi, Sorvall RC5C Plus, USA.

**Cuvette** Hellma, QH, QS, Germany.

**Deep Freeze** Bosch, -20°C, Turkey.

**dd$H_2O$** Millipore, MilliQ Academie, Elix-S, France.

**Digital Camera** Canon, PowerShot SD 400, USA; Olympus, C-7070, USA.

**Electrophoresis** BioRad Inc., USA; Novex, X Cell SureLock Electrophoresis Cell, USA.

**Element Analysis** Varian, Vista-Pro CCD Simultaneous ICP-OES, Australia; LECO, TruSpec CN, USA.

**Gel Documentation** BioRad, Universal Hood II, USA; BioRad, Quantity One, USA; BioRad, GelDoc XR, USA.

**Ice Machine** Scotsman Inc., AF20, USA.

**Imaging Software** GIMP 2.2.12.

**Incubator** Memmert D06059 Model 300, Germany.

**Incubator shaker** New Brunswick Scientific Innova 4330, USA.

**Laminar Flow Cabinets** Heraeus Instruments HS12, Germany.

**Lighting** Olympus, LG-PS2, USA.

**Magnetic Stir** VELP Scientifica, ARE Heating Magnetic Stirrer, Italy.

**Microliter Pipette** Gilson, Pipetman, France.

**Microplate Reader** BioRad, Model 680 Microplate Reader, USA.

**Microscope** Olympus, SZ61, USA.

**Microwave Oven** CEM Corp., Mars Xpress, USA; Bosch, Turkey.

**pH Meter** WTW, pH540GLP MultiCal, Germany.

**Power Supply** BioRad, PowerPac 300, USA; Wealtec, Elite 300, USA.

**Refrigirator** Bosch, +4°C, Turkey.

**Sonicator** Bioblock Scientific, Vibracell 75043, France; Bandelin, Sonorex, Germany.

**Spectrophotometer** Schimadzu, UV-3150, Japan; Nanodrop, ND-1000, USA.

**Thermomixer** Eppendorf, Thermomixer Comfort, Germany.

**Vortex** VELP Scientifica, $2x^3$, Italy.

## A.3 Additional data

### A.3.1 Element analysis

Table A.2: Creeping bentgrass ICP results

| Element | | Concentration (ppm) | | |
|---|---|---|---|---|
| | | 0 ppm Zn | 0.1 ppm Zn | 5 ppm Zn |
| P | Mean | 7325.49 | 6352.23 | 4056.95 |
| | StD | 699.17 | 680.44 | 222.61 |
| K | Mean | 22560.21 | 19846.16 | 18072.31 |
| | StD | 2095.58 | 1535.09 | 214.43 |
| Ca | Mean | 8155.27 | 7857.68 | 7420.45 |
| | StD | 1199.93 | 1029.88 | 635.08 |
| Mg | Mean | 3582.05 | 3539.73 | 2806.93 |
| | StD | 643.51 | 170.22 | 208.03 |
| S | Mean | 4224.07 | 4204.01 | 3096.18 |
| | StD | 246.50 | 244.48 | 292.03 |
| Fe | Mean | 131.04 | 119.76 | 57.49 |
| | StD | 29.18 | 14.53 | 5.95 |
| Mn | Mean | 212.94 | 200.51 | 120.29 |
| | StD | 52.01 | 27.00 | 9.74 |
| Cu | Mean | 20.29 | 18.20 | 12.69 |
| | StD | 4.05 | 2.03 | 1.21 |

Table A.3: Colonial bentgrass ICP results

| Element | | Concentration (ppm) | | |
|---|---|---|---|---|
| | | 0 ppm Zn | 0.1 ppm Zn | 5 ppm Zn |
| P | Mean | 6683.78 | 5161.54 | 3632.08 |
| | StD | 1343.51 | 594.67 | 423.19 |
| K | Mean | 2354.81 | 6231.11 | 26349.49 |
| | StD | 495.88 | 2800.20 | 1259.15 |
| Ca | Mean | 25602.88 | 15570.96 | 9580.72 |
| | StD | 5928.64 | 3026.88 | 2733.86 |
| Mg | Mean | 9573.96 | 6025.23 | 3669.41 |
| | StD | 572.73 | 574.55 | 394.93 |
| S | Mean | 4277.73 | 3324.93 | 3298.34 |
| | StD | 133.83 | 272.15 | 313.66 |
| Fe | Mean | 232.36 | 134.29 | 67.91 |
| | StD | 44.45 | 0.02 | 12.71 |
| Mn | Mean | 391.03 | 320.17 | 170.04 |
| | StD | 73.17 | 35.52 | 26.22 |
| Cu | Mean | 45.17 | 26.65 | 13.15 |
| | StD | 5.05 | 0.89 | 0.84 |

Table A.4: Velvet bentgrass ICP results

| Element | | Concentration (ppm) | | |
|---|---|---|---|---|
| | | 0 ppm Zn | 0.1 ppm Zn | 5 ppm Zn |
| P | Mean | 8169.83 | 6981.37 | 5888.90 |
| | StD | 2247.10 | 551.01 | 1767.72 |
| K | Mean | 16834.48 | 15077.71 | 24381.39 |
| | StD | 4465.75 | 1409.57 | 3369.47 |
| Ca | Mean | 16121.81 | 14594.06 | 8717.98 |
| | StD | 1129.79 | 3209.02 | 1993.81 |
| Mg | Mean | 5745.35 | 5717.59 | 3832.98 |
| | StD | 193.75 | 1602.83 | 738.37 |
| S | Mean | 3600.35 | 3393.60 | 3778.13 |
| | StD | 209.53 | 592.68 | 875.46 |
| Fe | Mean | 47.75 | 49.31 | 85.43 |
| | StD | 2.21 | 6.93 | 13.73 |
| Mn | Mean | 244.12 | 386.81 | 323.66 |
| | StD | 91.88 | 53.21 | 52.96 |
| Cu | Mean | 18.24 | 17.74 | 12.90 |
| | StD | 2.51 | 5.32 | 2.18 |